Robust Active and Passive Beamforming for RIS-Assisted Full-Duplex Systems under Imperfect CSI

Li-Hsiang Shen†, Chia-Jou Ku, and Kai-Ten Feng
†California PATH, University of California, Berkeley, USA
Department of Electronics and Electrical Engineering,
National Yang Ming Chiao Tung University, Hsinchu, Taiwan
shawngp3@berkeley.edu, chiajouku.ee09@nycu.edu.tw, and ktfeng@nycu.edu.tw

Abstract

The sixth-generation (6G) wireless technology recognizes the potential of reconfigurable intelligent surfaces (RIS) as an effective technique for intelligently manipulating channel paths through reflection to serve desired users. Full-duplex (FD) systems, enabling simultaneous transmission and reception from a base station (BS), offer the theoretical advantage of doubled spectrum efficiency. However, the presence of strong self-interference (SI) in FD systems significantly degrades performance, which can be mitigated by leveraging the capabilities of RIS. Moreover, accurately obtaining channel state information (CSI) from RIS poses a critical challenge. Our objective is to maximize downlink (DL) user data rates while ensuring quality-of-service (QoS) for uplink (UL) users under imperfect CSI from reflected channels. To address this, we introduce the robust active BS and passive RIS beamforming (RAPB) scheme for RIS-FD, accounting for both SI and imperfect CSI. RAPB incorporates distributionally robust design, conditional value-at-risk (CVaR), and penalty convex-concave programming (PCCP) techniques. Additionally, RAPB extends to active and passive beamforming (APB) with perfect channel estimation. Simulation results demonstrate the UL/DL rate improvements achieved considering various levels of imperfect CSI. The proposed RAPB/APB schemes validate their effectiveness across different RIS deployment and RIS/BS configurations. Benefited from robust beamforming, RAPB outperforms existing methods in terms of non-robustness, deployment without RIS, conventional successive convex approximation, and half-duplex systems.

Index Terms

RIS, FD, imperfect CSI, distributionally robust optimization, PCCP.

I. Introduction

The rapid development of wireless communications in the sixth-generation (6G) is driven by the increasing need for higher data rates, lower power consumption, and broader system coverage. To address these requirements, numerous emerging techniques are being developed for 6G wireless communications. One such technique is the reconfigurable intelligent surface (RIS) [1]–[3], which introduces a new hardware system to

assist in the implementation of 6G technologies. RIS is a passive surface consisting of independent massive meta-material based elements [4]. It possesses the capability to manipulate the phase-shifts of multiple passive reflecting elements, enabling the alteration of wireless propagation paths. As a result, RIS can provide a diverse multipath profile and redirect incident signals to desired users at specific locations. RIS is widely recognized for its high energy efficiency and flexible deployment, contributing to the improved signal quality and enhanced coverage across different domains, including device-to-device [5], non-orthogonal multiple access systems [6], vehicular communications [7], and multi-input-multi-output (MIMO) networks [8]. Furthermore, the joint design of active beamforming at transmitters and passive beamforming at RIS has emerged as a significant issue to be resolved. In [9], the authors focus on minimizing the symbol error rate by leveraging RIS functionality. The optimization of the RIS phase for maximizing energy efficiency is addressed in [10]. Additionally, the authors of [11] aim to minimize the overall power consumption of the base station (BS) by adjusting the configuration of the RIS. In [12], RISs are designed and optimized for enhancing the physical layer security to prevent information leakage to eavesdroppers. In [13], resource allocation is performed by employing RIS to diversify channels for both throughput-aware and latency-oriented users. The works in [14], [15] have demonstrated the prototypes to validate the feasibility effectiveness of RIS, including controller-based RIS and control-free RIS as a low cost version. Furthermore, an enhanced version of RIS capable of conducting joint reflection and refraction is recently becoming another powerful solution for extending wider coverage [16]. We notice that the implementation efficiency of converting the incident signals of RIS is still under development.

However, most of the existing works in this area have primarily focused on either uplink (UL) or downlink (DL) transmissions, potentially resulting in the underutilization of spectrum and channel diversity. To address this issue, full-duplex (FD) communication systems have emerged as a solution. FD transmission allows simultaneous transmission and reception of both DL and UL signals on the same frequency band, thereby doubling the spectrum efficiency compared to conventional half-duplex (HD) systems. However, the presence of strong self-interference (SI) imposes a significant challenge in FD systems, as it can degrade system quality. Several existing studies have addressed SI mitigation techniques. One study proposes a method based on oblique projection for nulling SI [17]. Another study focuses on resource allocation in FD networks considering the queue backlog of user equipment (UE) [18]. Optimal beamforming techniques to minimize SI power are derived through eigen-decomposition presented in [19]. However, these techniques require complex mechanisms and stringent assumptions about the base station (BS) due to the limited diversity of equipped antennas. Therefore, incorporating RIS and FD presents an alternative opportunity. RIS is capable of assisting FD networks in alleviating SI as well as inter-user interferences between UL and DL transmissions through destructive signals on reflective paths. In [20], relaying FD signals are accomplished with the assistance of RIS. In [21], resource allocation for spectral-efficient RIS-FD is conceived in non-

orthogonal multiple access. In [22], power minimization is considered with RISs possessing both reflection and refraction functionalities. The paper of [23] investigates scenarios where UE operates in HD mode, whilst the BS operates in FD mode. However, study of [24] impractically assume that the SI received at BS is well-known and eliminated.

However, most existing works on RIS-FD systems assume perfect knowledge of channel state information (CSI), which is impractical due to the limitations of RIS hardware. Since RIS is a passive surface without radio frequency or signal processing hardware, accurately estimating the CSI for the reflected channels through RIS is challenging. Therefore, research has focused on robust design approaches for RIS-aided systems, taking into account the random nature of the channels. However, most existing studies on robust RIS systems only consider two cases for modeling imperfect CSI. The first case is the Gaussian robust design, which assumes that the random channel variables follow a Gaussian distribution [25]. The second case is the worst-case robust design, which assumes a lower bound on the error distribution [26]. In the paper [27], Gaussian robust design has been applied to maximize the average UL sum-rate in RIS-aided systems, considering the impact of Doppler effect. Hybrid error models, including Gaussian distribution error and bounded error models, have been adopted in RIS-assisted multiple-input single-output (MISO) systems, demonstrating the superior performance of Gaussian robustness over the worst-case approach [28]. In [29], transmit power is minimized by optimizing transmit precoding and phase shifts at RIS, with the channel errors assumed to follow a Gaussian distribution and have norm-bounded characteristics. Furthermore, energy efficiency has been optimized in RIS-aided heterogeneous networks, considering bounded channel errors [30]. However, it is important to note that real channels may follow various distributions, and optimizing only for extreme conditions may sacrifice overall network performance. Therefore, it becomes compellingly imperative to explore more realistic and comprehensive error models for imperfect CSI in RIS-assisted systems.

As a remedy, distributionally robust design considers arbitrary channel distributions, making it more suitable for practical applications [31]. The works of [32], [33] optimize power balance and minimize transmit power using distributionally robust design. In [34], the authors apply distributionally robust design to secure optimization. Additionally, [35] considers both Gaussian robust design and distributionally robust design in MIMO systems, demonstrating that distributionally robust design outperforms Gaussian robust design. Note that the existing literature has not extensively explored distributionally robust design in RIS-aided systems. Motivated by the aforementioned studies, this is the first work to investigate robust RIS optimization relying on arbitrary distribution of imperfect CSI on RIS channels. As an extension of our previous work of [36], we incorporate both active beamforming at BS and passive RIS beamforming in RIS-FD systems with imperfect CSI. The contributions of this work can be summarized as follows.

- We formulate a DL rate maximization problem while guaranteeing UL quality-of-service (QoS) for

RIS-FD systems. We consider the constraints of active beamforming power of BS and RIS phase-shift configuration. We propose the robust active BS and passive RIS beamforming (RAPB) scheme considering imperfect CSI of the cascaded RIS channel between BS and RIS, as well as the RIS and UE. Additionally, we extend RAPB to active and passive beamforming (APB) under well-estimated perfect channel status. Note that RAPB has a higher computational complexity order than that of APB due to robustness processing.

- In RAPB, random RIS channel error is considered and resolved through distributionally robust design, which requires only the mean and covariance of any error distribution. We decouple the original non-convex non-linear stochastic problem to two subproblems respectively optimizing BS beamforming and RIS configuration. The conditional value-at-risk (CVaR) is employed to deal with robust DL/UL rate optimizations. Moreover, general sign-definiteness principle and Schur complements are adopted to optimize BS/RIS configurations. As last, we leverage linear matrix inequality (LMI) to iteratively solve two subproblems until convergence.
- In APB, the error-free RIS channel is assumed. By applying Lagrangian dual and Dinkelbach transform, the logarithms and fractional objective functions are resolved. Similarly, the original problem is decoupled into the two subproblems, which are iteratively solved until convergence. We incorporate successive convex approximation (SCA) and penalty convex-concave programming (PCCP) to tackle the non-convex functions and phase-shift constraints, respectively.
- We evaluate the system performance of our proposed RAPB method and APB schemes. Through simulations, we analyze the convergence, effectiveness, and robustness of both robust and non-robust designs. Our results indicate that simply increasing the number of RIS reflecting elements does not guarantee improved system performance. In cases where the error variance of the reflected channel is extremely high, it deteriorates the performance of RIS-FD systems. However, RAPB exhibits robustness against random channel errors and sustains acceptable rate performance. Furthermore, benefited from robust beamforming, RAPB outperforms existing methods in terms of non-robustness, deployment without RIS, conventional successive convex approximation, and half-duplex systems.

II. System Model and Problem Formulation

A. Signal Model

As illustrated in Fig. 1, we consider an RIS-assisted FD network, including an FD-enabled BS, a deployed RIS, and M DL UEs as well as N UL UEs with respective UE set as $\mathcal{M} = \{1, 2, ..., M\}$ and $\mathcal{N} = \{1, 2, ..., N\}$. Note that all UEs operate in HD mode for either UL or DL direction. The BS is equipped with N_t DL transmit antennas (Tx) and N_r receiving UL antennas (Rx), whereas the RIS possesses K reflecting elements with their respective sets of $\mathcal{N}_t$, $\mathcal{N}_r$ and $\mathcal{K}$. Each UE is assumed to be equipped with a single

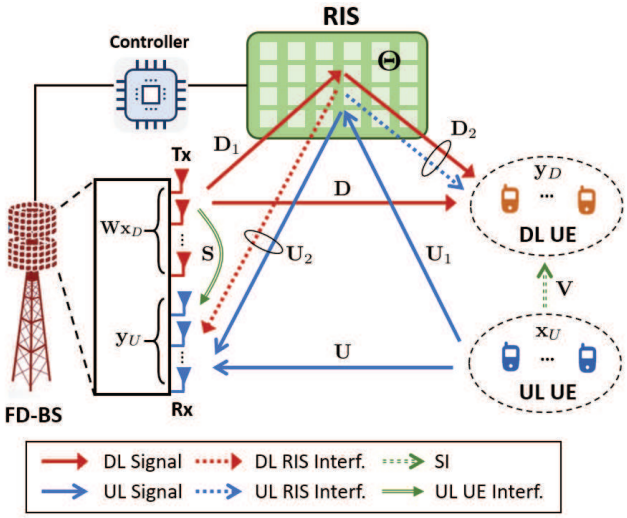

Fig. 1. Architecture of RIS-FD network with an FD-BS with UL/DL UEs in HD mode. An RIS controlled by the BS is deployed to reflect both UL/DL signals at same frequency band.

antenna. As for UL, $\mathbf{U} \in \mathbb{C}^{N_r \times N}$ indicates the direct path from UL UEs to BS receiving antennas, whilst the reflected paths from UL UEs to RIS and from RIS to BS are defined as $\mathbf{U}_1 \in \mathbb{C}^{K \times N}$ and $\mathbf{U}_2 \in \mathbb{C}^{N_r \times K}$, respectively. As for DL, $\mathbf{D} \in \mathbb{C}^{M \times N_t}$ denotes the direct path from BS transmit antennas to DL UEs, whilst the reflected paths from BS transmit antennas to RIS and from RIS to DL UEs are defined as $\mathbf{D}_1 \in \mathbb{C}^{K \times N_t}$ and $\mathbf{D}_2 \in \mathbb{C}^{M \times K}$ represents the channel from RIS to DL UE, respectively. $\mathbf{S} \in \mathbb{C}^{N_r \times N_t}$ denotes the SI channel induced by from BS transmit antennas to received ones, whilst $\mathbf{V} \in \mathbb{C}^{M \times N}$ stands for the co-channel interference from UL to DL UEs. As for RIS, we define $\mathbf{\Theta} = \text{diag}\left(\beta_1 e^{j\theta_1}, ..., \beta_k e^{j\theta_k}, ..., \beta_K e^{j\theta_K}\right) \in \mathbb{C}^{K \times K}$ as the RIS reflection matrix, where β_k is the RIS amplitude and $e^{j\theta_k}$ is the reflection phase shift with a range of $\theta_k \in [0, 2\pi)$. Note that we consider RIS with whole reflection of the incident signal power, i.e., $\beta_k = 1, \forall k$. Therefore, the received DL signal of DL UE m is given by

$$y_m = \underbrace{\sqrt{p_D}\left(\mathbf{D}_m + \mathbf{D}_{2,m}\mathbf{\Theta}\mathbf{D}_1\right)\mathbf{w}_m x_{D,m}}_{\text{Downlink Signal}} + \underbrace{\sqrt{p_U}(\mathbf{V}_m + \mathbf{D}_{2,m}\mathbf{\Theta}\mathbf{U}_1)\mathbf{x}_U}_{\text{Co-Channel Interference}} + \sum_{m' \in \mathcal{M} \setminus m} \underbrace{\sqrt{p_D}(\mathbf{D}_m + \mathbf{D}_{2,m}\mathbf{\Theta}\mathbf{D}_1)\mathbf{w}_{m'} x_{D,m'}}_{\text{Inter-DL UE Interference}} + n_m, \tag{1}$$

where p_D and p_U indicate transmit power of DL BS and UL UE, respectively. In (1), $\mathbf{D}_m \in \mathbb{C}^{1 \times N_t}$ and $\mathbf{D}_{2,m} \in \mathbb{C}^{1 \times K}$ denote the m-th row vector in $\mathbf{D}$ and $\mathbf{D}_2$ for the channels from BS and from RIS to DL UE m, respectively. Also, $\mathbf{V}_m \in \mathbb{C}^{1 \times N}$ is for co-channel interference from UL UEs to DL UE m. Notation of $\mathbf{W} = [\mathbf{w}_1, ..., \mathbf{w}_m, ..., \mathbf{w}_M] \in \mathbb{C}^{N_t \times M}$ is the precoding matrix in the beamforming-enabled transmit antennas at BS, where $\mathbf{w}_m \in \mathbb{C}^{N_t}$ is the precoding vector associated with DL UE m. Note that $\mathbf{x}_D = [x_{D,1}, ..., x_{D,m}, ..., x_{D,M}]^{\mathcal{T}} \in \mathbb{C}^M$ and $\mathbf{x}_U = [x_{U,1}, ..., x_{U,n}, ..., x_{U,N}]^{\mathcal{T}} \in \mathbb{C}^N$ are defined as the data stream at transmit antennas of DL BS and of UL UE, respectively. Note that $\mathcal{T}$ is the transpose operation. Notation $n_m \sim \mathcal{CN}(0, \sigma_m^2)$ is the additive white Gaussian noise (AWGN) with zero mean and variance σ_m^2.

Moreover, the received UL signal at receiving antennas of the BS is expressed as

$$\mathbf{y}_U = \underbrace{\sqrt{p_U}(\mathbf{U} + \mathbf{U}_2\boldsymbol{\Theta}\mathbf{U}_1)\mathbf{x}_U}_{\text{Uplink Signal}} + \underbrace{\sqrt{p_D}(\mathbf{S} + \mathbf{U}_2\boldsymbol{\Theta}\mathbf{D}_1)\mathbf{W}\mathbf{x}_D}_{\text{Self-Interference}} + \mathbf{n}_U, \tag{2}$$

where $\mathbf{n}_U \sim \mathcal{CN}(\mathbf{0}, \sigma_U^2\mathbf{e}_{N_r})$ is AWGN noise, where $\mathbf{0}$ is zero-mean vector with length N_r, σ_U^2 indicate UL noise power, and $\mathbf{e}_{N_r}$ is the unit vector with length N_r. In (1), interferences come from co-channel interferences (CCI) from UL UEs to DL ones, whilst inter-DL interference is from the superposed signals at BS Tx. In (2), the only interference is induced from SI from BS Tx to its Rx. Different from conventional non-RIS network, we notice additional reflective interferences appear in both CCI and SI. Note that $\boldsymbol{\Theta}$ is coupled in between two cascaded reflecting channels, which leads to a difficulty to the following derivation. Accordingly, we rewrite the simplified received signals as

$$y_m = \sqrt{p_D}\left(\mathbf{D}_m + \mathbf{D}_{t_m}\boldsymbol{\Theta}^{(D)}\right)\mathbf{w}_m x_{D,m} + \sqrt{p_U}\left(\mathbf{V}_m + \mathbf{C}_{t_m}\boldsymbol{\Theta}^{(U)}\right)\mathbf{x}_U + \sum_{m' \in \mathcal{M}\setminus m}\sqrt{p_D}\left(\mathbf{D}_m + \mathbf{D}_{t_m}\boldsymbol{\Theta}^{(D)}\right)\mathbf{w}_{m'}x_{D,m'} + n_m, \tag{3}$$

$$\mathbf{y}_U = \sqrt{p_U}\left(\mathbf{U} + \mathbf{U}_t\boldsymbol{\Theta}^{(U)}\right)\mathbf{x}_U + \sqrt{p_D}\left(\mathbf{S} + \mathbf{S}_t\boldsymbol{\Theta}^{(D)}\right)\mathbf{W}\mathbf{x}_D + \mathbf{n}_U, \tag{4}$$

where we define $\boldsymbol{\Theta}^{(D)} = [\mathbf{E}_{D,1}, \mathbf{E}_{D,2}, ..., \mathbf{E}_{D,K}]^{\mathcal{T}}$ and $\boldsymbol{\Theta}^{(U)} = [\mathbf{E}_{U,1}, \mathbf{E}_{U,2}, ..., \mathbf{E}_{U,K}]^{\mathcal{T}}$, where $\mathbf{E}_{D,k} = e^{j\theta_k}\mathbf{I}_{N_t} \in \mathbb{C}^{N_t \times N_t}$ and $\mathbf{E}_{U,k} = e^{j\theta_k}\mathbf{I}_N \in \mathbb{C}^{N \times N}$ with $\mathbf{I}_{N_t}$ and $\mathbf{I}_N$ as identity matrix. In (3), we define $\mathbf{D}_{t_m} = [\mathbf{D}_{2,m,1}\mathbf{D}_{1,1}, ..., \mathbf{D}_{2,m,k}\mathbf{D}_{1,k}, ..., \mathbf{D}_{2,m,K}\mathbf{D}_{1,K}] \in \mathbb{C}^{1 \times KN_t}$ as the cascaded channel from BS Tx, RIS, to DL UE m, where $\mathbf{D}_{2,m,k} \in \mathbb{C}$ is the scalar element in the m-th row and k-th column of $\mathbf{D}_2$, and $\mathbf{D}_{1,k} \in \mathbb{C}^{1 \times N_t}$ is the k-th row vector of $\mathbf{D}_1$. Notation of $\mathbf{C}_{t_m} = [\mathbf{D}_{2,m,1}\mathbf{U}_{1,1}, ..., \mathbf{D}_{2,m,k}\mathbf{U}_{1,k}, ..., \mathbf{D}_{2,m,K}\mathbf{U}_{1,K}] \in \mathbb{C}^{1 \times KN}$ denotes the cascaded CCI channel from UL UE, RIS, to DL UE m, where $\mathbf{U}_{1,k} \in \mathbb{C}^{1 \times N}$ is the k-th row vector of $\mathbf{U}_1$. In (4), we define $\mathbf{U}_t = [\mathbf{U}_{2,1}\mathbf{U}_{1,1}, ...\mathbf{U}_{2,k}\mathbf{U}_{1,k}, ..., \mathbf{U}_{2,K}\mathbf{U}_{1,K}] \in \mathbb{C}^{N_r \times KN}$ as the cascaded channel from UL UE, RIS, to BS Rx, where $\mathbf{U}_{2,k} \in \mathbb{C}^{N_r}$ is the k-th column vector of $\mathbf{U}_2$, and $\mathbf{U}_{1,k} \in \mathbb{C}^N$ is the k-th row vector of $\mathbf{U}_1$. Notation of $\mathbf{S}_t = [\mathbf{U}_{2,1}\mathbf{D}_{1,1}, ..., \mathbf{U}_{2,k}\mathbf{D}_{1,k}, ..., \mathbf{U}_{2,K}\mathbf{D}_{1,K}] \in \mathbb{C}^{N_r \times KN_t}$ denotes the cascaded SI channel from BS Tx, RIS to BS Rx, where $\mathbf{D}_{1_K} \in \mathbb{C}^{N_t}$ is the k-th row vector of $\mathbf{D}_1$.

B. Imperfect CSI Model

We consider the imperfect estimation of CSI for RIS due to its passive nature, which requires robust optimization to account for such imperfections. These imperfections can arise from factors such as estimation errors, time-varying effects, asynchronous transmission delays, and hardware impairments. Most existing papers either consider an impractical assumption of Gaussian distribution or focus on worst-case guarantees. In this paper, we only consider the first and second moments of the imperfect CSI, i.e., the mean and variance of the arbitrary channel distribution, as the attainable information. Moreover, we assume that the

RIS channel for reflection is subject to imperfect CSI, whilst the other channels can be well-estimated by the BS. Therefore, the reflected imperfect channels in our system can be modeled as

$$\mathbf{D}_{t_m} = \widetilde{\mathbf{D}}_{t_m} + \triangle\mathbf{D}_{t_m}, \quad \mathbf{C}_{t_m} = \widetilde{\mathbf{C}}_{t_m} + \triangle\mathbf{C}_{t_m}, \quad \mathbf{U}_t = \widetilde{\mathbf{U}}_t + \triangle\mathbf{U}_t, \quad \mathbf{S}_t = \widetilde{\mathbf{S}}_t + \triangle\mathbf{S}_t, \tag{5}$$

where $\widetilde{\mathbf{D}}_{t_m}$, $\widetilde{\mathbf{C}}_{t_m}$, $\widetilde{\mathbf{U}}_t$ and $\widetilde{\mathbf{S}}_t$ are the estimated reflected channel for $\mathbf{D}_{t_m}$, $\mathbf{C}_{t_m}$, $\mathbf{U}_t$ and $\mathbf{S}_t$, respectively. $\triangle\mathbf{D}_{t_m}$, $\triangle\mathbf{C}_{t_m}$, $\triangle\mathbf{U}_t$ and $\triangle\mathbf{S}_t$ are the corresponding random channel error. The mean and variance for imperfect CSI regarding real $\mathrm{Re}\{\cdot\}$ and image $\mathrm{Im}\{\cdot\}$ part are respectively expressed as

$$\begin{aligned}
&\mathbb{E}_{\mathfrak{D}}\{\mathrm{Re}\{\triangle\mathbf{D}_{t_m}\}\} = \mathbb{E}_{\mathfrak{D}}\{\mathrm{Im}\{\triangle\mathbf{D}_{t_m}\}\} = \boldsymbol{\mu}_m^{(D)}, \quad \mathbb{E}_{\mathfrak{D}}\{\mathrm{Re}\{\triangle\mathbf{C}_{t_m}\}\} = \mathbb{E}_{\mathfrak{D}}\{\mathrm{Im}\{\triangle\mathbf{C}_{t_m}\}\} = \boldsymbol{\mu}_m^{(C)}, \\
&\mathbb{E}_{\mathfrak{D}}\{\mathrm{Re}\{\triangle\mathbf{U}_t\}\} = \mathbb{E}_{\mathfrak{D}}\{\mathrm{Im}\{\triangle\mathbf{U}_t\}\} = \boldsymbol{\mu}^{(U)}, \quad \mathbb{E}_{\mathfrak{D}}\{\mathrm{Re}\{\triangle\mathbf{S}_t\}\} = \mathbb{E}_{\mathfrak{D}}\{\mathrm{Im}\{\triangle\mathbf{S}_t\}\} = \boldsymbol{\mu}^{(S)},
\end{aligned} \tag{6}$$

and

$$\begin{aligned}
&\mathbb{E}_{\mathfrak{D}}\{(\mathrm{Re}\{\triangle\mathbf{D}_{t_m}\})^2\} = \mathbb{E}_{\mathfrak{D}}\{(\mathrm{Im}\{\triangle\mathbf{D}_{t_m}\})^2\} = \delta\boldsymbol{\Sigma}_m^{(D)}, \mathbb{E}_{\mathfrak{D}}\{(\mathrm{Re}\{\triangle\mathbf{C}_{t_m}\})^2\} = \mathbb{E}_{\mathfrak{D}}\{(\mathrm{Im}\{\triangle\mathbf{C}_{t_m}\})^2\} = \delta\boldsymbol{\Sigma}_m^{(C)}, \\
&\mathbb{E}_{\mathfrak{D}}\{(\mathrm{Re}\{\triangle\mathbf{U}_t\})^2\} = \mathbb{E}_{\mathfrak{D}}\{(\mathrm{Im}\{\triangle\mathbf{U}_t\})^2\} = \delta\boldsymbol{\Sigma}^{(U)}, \quad \mathbb{E}_{\mathfrak{D}}\{(\mathrm{Re}\{\triangle\mathbf{S}_t\})^2\} = \mathbb{E}_{\mathfrak{D}}\{(\mathrm{Im}\{\triangle\mathbf{S}_t\})^2\} = \delta\boldsymbol{\Sigma}^{(S)},
\end{aligned} \tag{7}$$

where $\mathbb{E}_{\mathfrak{D}}[\cdot]$ stands for the statistical expectation under the distribution of $\mathfrak{D}$. The symbols $\boldsymbol{\mu}^{(\cdot)}$ and $\boldsymbol{\Sigma}^{(\cdot)}$ respectively denote the mean and variance matrix, whereas $\boldsymbol{\mu}_m^{(\cdot)}$ and $\boldsymbol{\Sigma}_m^{(\cdot)}$ indicate the vector representations. Note that δ indicates the scaling constant for the level of error variance.

Therefore, the signal-to-interference-plus-noise ratio (SINR) of DL UE m and of UL BS receiving antennas for UL UE n are respectively represented as

$$\mathrm{SINR}_{D,m} = \frac{\|(\mathbf{D}_m + \mathbf{D}_{t_m}\boldsymbol{\Theta}^{(D)})\mathbf{w}_m\overline{x}_{D,m}\|^2}{\sum\limits_{m'\in\mathcal{M}\setminus m}\|(\mathbf{D}_m + \mathbf{D}_{t_m}\boldsymbol{\Theta}^{(D)})\mathbf{w}_{m'}\overline{x}_{D,m'}\|^2 + \|(\mathbf{V}_m + \mathbf{C}_{t_m}\boldsymbol{\Theta}^{(U)})\overline{\mathbf{x}}_U\|^2 + \sigma^2} \triangleq \frac{D_{S,m}(\boldsymbol{\Theta},\mathbf{W})}{D_{I,m}(\boldsymbol{\Theta},\mathbf{W}) + D_{C,m}(\boldsymbol{\Theta}) + \sigma^2}, \tag{8}$$

$$\mathrm{SINR}_{U,n} = \frac{\|(\mathbf{U}_n + \mathbf{U}_{t,n}\boldsymbol{\Theta}_n^{(U)})\overline{x}_{U,n}\|^2}{\|(\mathbf{S} + \mathbf{S}_t\boldsymbol{\Theta}^{(D)})\mathbf{W}\overline{\mathbf{x}}_D\|^2 + \sigma^2} \triangleq \frac{U_{S,n}(\boldsymbol{\Theta})}{U_{I,n}(\boldsymbol{\Theta},\mathbf{W}) + \sigma^2}, \tag{9}$$

where $\overline{x}_{D,m} = \sqrt{p_D}x_{D,m}, \forall m \in \mathcal{M}$, $\overline{x}_{U,n} = \sqrt{p_U}x_{U,n}, \forall n \in \mathcal{N}$, $\overline{\mathbf{x}}_D = \sqrt{p_D}\mathbf{x}_D$, and $\overline{\mathbf{x}}_U = \sqrt{p_U}\mathbf{x}_U$. We consider equivalent noise power for all UEs denoted as σ^2. Note that we omit the repeated definitions of symbols in both the denominator and numerator terms in the rightmost expressions of (8) and (9). The DL/UL user data rate can be respectively attained as

$$R_{D,m}(\boldsymbol{\Theta},\mathbf{W}) = \log_2(1 + \mathrm{SINR}_{D,m}), \quad R_{U,n}(\boldsymbol{\Theta},\mathbf{W}) = \log_2(1 + \mathrm{SINR}_{U,n}). \tag{10}$$

C. Problem Formulation

We consider a optimization problem with the arguments of active BS beamforming $\mathbf{W}$ and passive RIS beamforming $\boldsymbol{\Theta}$. We aim at performing the maximization of total system DL rate while guaranteeing UL

QoS of total system UL rate, which can be represented by

$$\max_{\mathbf{\Theta},\mathbf{W}} \sum_{m\in\mathcal{M}} R_{D,m}(\mathbf{\Theta},\mathbf{W}) \tag{11a}$$

$$\text{s.t.} \sum_{n\in\mathcal{N}} R_{U,n}(\mathbf{\Theta},\mathbf{W}) \geq t_{th,U}, \tag{11b}$$

$$\left|e^{j\theta_k}\right|^2 = 1, \quad \forall k \in \mathcal{K}, \tag{11c}$$

$$\sum_{m\in\mathcal{M}} \mathbf{w}_m^{\mathcal{H}}\mathbf{w}_m \leq P_{\max}. \tag{11d}$$

The constraint (11b) indicates that system UL data rate should be higher than a given threshold $t_{th,U}$. The constraint (11c) stands for RIS configuration, whilst (11d) is for the maximum allowable BS transmit power of $P_{\max}$. $\mathcal{H}$ denotes the Hermitian operation of a matrix. As observed from (11), we can infer that both the objective and constraints are non-convex and non-linear, involving fractional functions in logarithmic expressions and the equality constraint of RIS. Additionally, the presence of imperfect CSI in the stochastic problem further complicates the optimization task. In the following, we first address the optimization problem assuming perfect CSI, and then we consider the robust optimization problem taking into account imperfect CSI.

III. Proposed APB Scheme with Perfect CSI

In the case of perfect CSI, we consider $\triangle\mathbf{D}_{t_m} = \triangle\mathbf{C}_{t_m} = \triangle\mathbf{U}_t = \triangle\mathbf{S}_t = 0$. In order to tackle this complex problem, we have to deal with logarithmic and fractional functions with the coupled variables, and constraints and the non-convex equations. Therefore, we adopt alternative algorithm (AO) which optimizes subproblems in an alternative manner. The problem (11) is decomposed into two subproblems, including passive RIS and active BS beamforming. The detailed flowchart of a series of problem transformation of APB is depicted in Fig. 2. We will elaborate the respective blocks as follows.

A. Logarithmic and Fractional Transformation

We can observe that the objective function performs summation of logarithmic functions with each having fractional expression of SINR. To tackle the issues, we employ Lagrangian dual transform [37] and the Dinkelbach method [38]. Firstly, we transform the constraint of (11b) due to multiple summation operations. Based on Jensen's inequality, we have a lower bound of total UL rate bound as $\sum_{n\in\mathcal{N}} R_{U,n}(\mathbf{\Theta},\mathbf{W}) \geq R_U(\mathbf{\Theta},\mathbf{W}) = \log_2(1+\text{SINR}_U)$, where $\text{SINR}_U = \frac{\|(\mathbf{U}+\mathbf{U}_t\mathbf{\Theta}^{(U)})\overline{\mathbf{x}}_U\|^2}{\|(\mathbf{S}+\mathbf{S}_t\mathbf{\Theta}^{(U)})\mathbf{W}\overline{\mathbf{x}}_D\|^2+\sigma^2} \triangleq \frac{U_S(\mathbf{\Theta})}{U_I(\mathbf{\Theta},\mathbf{W})+\sigma^2}$ is the equivalent

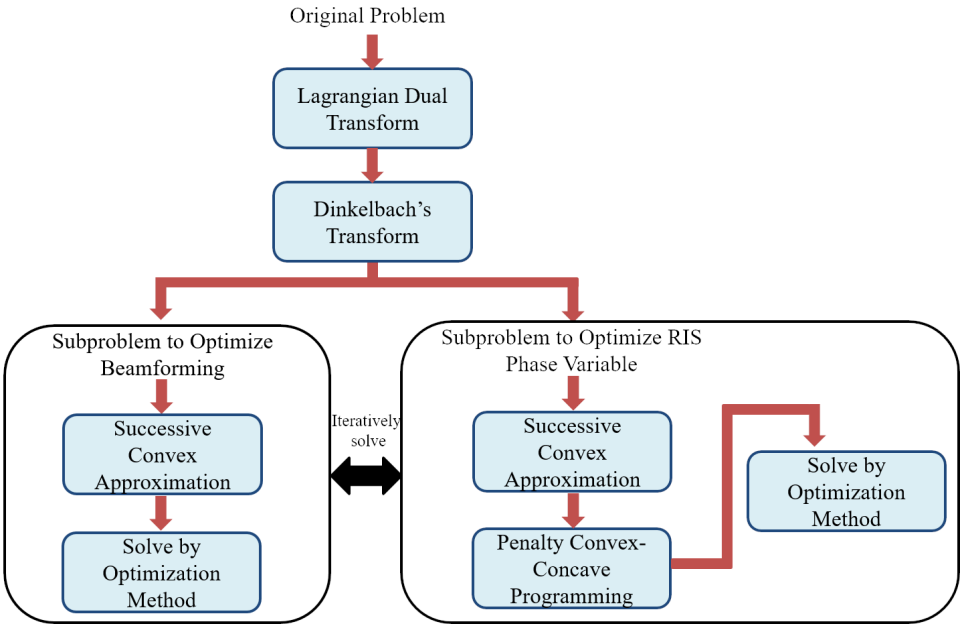

Fig. 2. Flowchart of non-robust problem transformation.

expression of total SINR of UL UEs. Therefore, the transformed problem of (11) is given by

$$\max_{\boldsymbol{\Theta},\mathbf{W}} \sum_{m\in\mathcal{M}} R_{D,m}(\boldsymbol{\Theta},\mathbf{W}) \tag{12a}$$

$$\text{s.t. } R_U(\boldsymbol{\Theta},\mathbf{W}) \geq t_{th,U}, \tag{12b}$$

$$(11c), (11d). \tag{12c}$$

In the following proposition, we design to remove the logarithmic function in (12a).

Proposition 1. *The sum-of-logarithm problem* (12) *is equivalent to solving*

$$\max_{\boldsymbol{\Theta},\mathbf{W}} \overline{F}_D(\boldsymbol{\Theta},\mathbf{W}) = \sum_{m\in\mathcal{M}} \frac{(1+r_m^*)D_{S,m}(\boldsymbol{\Theta},\mathbf{W})}{D_{S,m}(\boldsymbol{\Theta},\mathbf{W})+D_{I,m}(\boldsymbol{\Theta},\mathbf{W})+D_{C,m}(\boldsymbol{\Theta})+\sigma^2} \tag{13a}$$

$$\text{s.t. } (11c), (11d), (12b), \tag{13b}$$

where $r_m^* = \frac{D_{S,m}(\boldsymbol{\Theta},\mathbf{W})}{D_{I,m}(\boldsymbol{\Theta},\mathbf{W})+D_{C,m}(\boldsymbol{\Theta})+\sigma^2}$ *is auxiliary term corresponding to the optimal DL SINR.*

Proof. Based on Lagrangian dual transform, we have weighted sum-of-logarithms given by

$$F_D(\boldsymbol{\Theta},\mathbf{W},\boldsymbol{r}) = \sum_{m\in\mathcal{M}} \log_2(1+r_m) - \sum_{m\in\mathcal{M}} r_m + \sum_{m\in\mathcal{M}} \frac{(1+r_m)D_{s,m}(\boldsymbol{\Theta},\mathbf{W})}{D_{S,m}(\boldsymbol{\Theta},\mathbf{W})+D_{I,m}(\boldsymbol{\Theta},\mathbf{W})+D_{C,m}(\boldsymbol{\Theta})+\sigma^2}$$

where $\boldsymbol{r} = [r_1, r_2, ..., r_M]$ indicates the auxiliary variable of DL SINR. We can observe that $F_D(\boldsymbol{\Theta},\mathbf{W},\boldsymbol{r})$ is convex and differentiable function with respect to (w.r.t.) r_m^* with fixed BS/RIS parameters $\{\boldsymbol{\Theta},\mathbf{W}\}$.

Therefore, the optimum of r_m^* can be obtained by $\frac{\partial F_D(\mathbf{\Theta},\mathbf{W},\boldsymbol{r})}{\partial r_m}=0$. Substituting r_m^* in $F_D(\mathbf{\Theta},\mathbf{W},\boldsymbol{r})$ yields (13a). This completes the proof. □

Note that r_m^* can be set as the optimum of DL SINR acquired at previous iteration. We employ the Dinkelbach method in (13a), which converts the fractional expression into an affine function as

$$\widetilde{F}_D(\mathbf{\Theta},\mathbf{W})=\sum_{m\in\mathcal{M}}(1+r_m^*)D_{S,m}(\mathbf{\Theta},\mathbf{W})-t_m^*\left(D_{S,m}(\mathbf{\Theta},\mathbf{W})+D_{I,m}(\mathbf{\Theta},\mathbf{W})+D_{C,m}(\mathbf{\Theta})+\sigma^2\right), \tag{14}$$

where the optimal solution of the Lagrangian dual in the i-th iteration is defined as the optimum obtained in the previous iteration denoted by

$$t_m^*=\frac{(1+r_m^*)D_{s,m}(\mathbf{\Theta}^{*(i-1)},\mathbf{W}^{*(i-1)})}{D_{S,m}(\mathbf{\Theta}^{*(i-1)},\mathbf{W}^{*(i-1)})+D_{I,m}(\mathbf{\Theta}^{*(i-1)},\mathbf{W}^{*(i-1)})+D_{C,m}(\mathbf{\Theta}^{*(i-1)})+\sigma^2}. \tag{15}$$

Moreover, UL QoS in (12b) can be rewritten as

$$\text{SINR}_U\geq\overline{t}_{th,U}\ \Rightarrow\ U_S(\mathbf{\Theta})\geq\overline{t}_{th,U}(U_I(\mathbf{\Theta},\mathbf{W})+\sigma^2), \tag{16}$$

where $\overline{t}_{th,U}=2^{t_{th,U}}-1$. In the last inequality, the denominator of SINR is moved to the right-hand side. Therefore, the problem (13) in the i-th iteration can be acquired as

$$\max_{\mathbf{\Theta},\mathbf{W}}\ \widetilde{F}_D(\mathbf{\Theta},\mathbf{W}) \tag{17a}$$

$$\text{s.t. (11c), (11d), (16).} \tag{17b}$$

However, we can infer that the problem (17) still performs non-convexity and non-linearity due to coupled variables of $\{\mathbf{\Theta},\mathbf{W}\}$. Therefore, we decouple the problem (17) into two subproblems by AO algorithm, including active BS beamforming and passive RIS phase shifts, which are elaborated as follows.

B. Alternative Optimization

1) Optimization of Active BS Transmit Beamforming: While the RIS phase matrix $\mathbf{\Theta}^*$ is fixed, problem (17) is reduced to

$$\max_{\mathbf{W}}\ \widetilde{F}_D^w(\mathbf{W})=\sum_{m\in\mathcal{M}}(1+r_m^*)D_{S,m}(\mathbf{W})-t_m^*(D_{t,m}(\mathbf{W})+n_m) \tag{18a}$$

$$\text{s.t. (11d)},\ U_I(\mathbf{W})\leq\xi_U, \tag{18b}$$

where $D_{S,m}(\mathbf{W})=\|(\mathbf{D}_m+\mathbf{D}_{t_m}\mathbf{\Theta}^{*(D)})\mathbf{w}_m\overline{x}_{D,m}\|^2\triangleq\|\mathbf{D}_{w,m}\mathbf{w}_m\|^2$, $D_{t,m}(\mathbf{W})=\sum_{m'\in\mathcal{M}}\|(\mathbf{D}_m+\mathbf{D}_{t_m}\mathbf{\Theta}^{*(D)})\mathbf{w}_{m'}\overline{x}_{D,m'}\|^2\triangleq\sum_{m'\in\mathcal{M}}\|\mathbf{D}_{w,m}\mathbf{w}_{m'}\|^2$, and $n_m=D_{C,m}(\mathbf{\Theta}^*)+\sigma^2$. By moving beamforming parameters to the left-hand side of inequality in (16), we have $U_I(\mathbf{W})=\|(\mathbf{S}+\mathbf{S}_t\mathbf{\Theta}^{*(D)})\mathbf{W}\overline{\mathbf{x}}_D\|^2\triangleq$

$\|\mathbf{S}_w \sum_{m\in\mathcal{M}} \mathbf{w}_m\|^2$ and $\xi_U = \frac{U_S(\mathbf{\Theta}^*)-\bar{t}_{th,U}\sigma^2}{\bar{t}_{th,U}}$. Note that these terms are related to only beamforming parameter $\mathbf{W}$ with the fixed optimal RIS solution of $\mathbf{\Theta}^*$.

Now, the DL/UL terms related to beamforming in problem (18) can be further expressed as quadratic form. The DL objective in (18a) is expressed as

$$\widetilde{F}_D(\mathbf{W}) = \sum_{m\in\mathcal{M}} \mathbf{w}_m^{\mathcal{H}} \mathbf{\Omega}_{w,m} \mathbf{w}_m - t_m^* \left(\sum_{m'\in\mathcal{M}} \mathbf{w}_{m'}^{\mathcal{H}} \mathbf{\Omega}_{w,m} \mathbf{w}_{m'} + n_m \right), \tag{19}$$

where $\mathbf{\Omega}_{w,m} = (1 + r_m^*)\mathbf{D}_{w,m}^{\mathcal{H}} \mathbf{D}_{w,m}$. As for UL QoS in (18b), we have

$$U_I(\mathbf{W}) = \sum_{m\in\mathcal{M}} \mathbf{w}_m^{\mathcal{H}} \mathbf{\Omega}_{w,U} \sum_{m\in\mathcal{M}} \mathbf{w}_m = \sum_{m\in\mathcal{M}} \mathbf{w}_m^{\mathcal{H}} \mathbf{\Omega}_{w,U} \mathbf{w}_m + 2 \sum_{m=1}^{M-1} \sum_{m'=m+1}^{M} \mathbf{w}_m^{\mathcal{H}} \mathbf{\Omega}_{w,U} \mathbf{w}_{m'} \leq \xi_U, \tag{20}$$

where $\mathbf{\Omega}_{w,U} = \mathbf{S}_w^{\mathcal{H}} \mathbf{S}_w$. However, the objective (19) performs a convex-concave function, whilst beamforming variables are coupled in (20). Therefore, SCA is employed to transform the non-convex term to convex one. Based on the first-order Taylor approximation, we can acquire the alternative lower bounds as

$$\mathbf{w}_m^{\mathcal{H}} \mathbf{\Omega}_{w,m} \mathbf{w}_m \geq 2\mathrm{Re}\{(\mathbf{w}_m^{(p)})^{\mathcal{H}} \mathbf{\Omega}_{w,m} \mathbf{w}_m\} - (\mathbf{w}_m^{(p)})^{\mathcal{H}} \mathbf{\Omega}_{w,m} \mathbf{w}_m^{(p)} \tag{21}$$

$$\sum_{m=1}^{M-1} \sum_{m'=m+1}^{M} \mathbf{w}_m^{\mathcal{H}} \mathbf{\Omega}_{w,U} \mathbf{w}_{m'} \geq \sum_{m=1}^{M-1} \sum_{m'=m+1}^{M} 2\mathrm{Re}\{(\mathbf{w}_m^{(p)})^{\mathcal{H}} \mathbf{\Omega}_{w,U} \mathbf{w}_{m'}\} - (\mathbf{w}_m^{(p)})^{\mathcal{H}} \mathbf{\Omega}_{w,U} \mathbf{w}_{m'}^{(p)}. \tag{22}$$

We define $\mathbf{w}_m^{(p)}$ as a constant solution of active beamforming obtained at iteration p. Based on (19) and (21), the objective of (18a) is transformed into

$$\widetilde{F}_{D,t}(\mathbf{W}) = \sum_{m\in\mathcal{M}} -t_m^* \left(\sum_{m'\in\mathcal{M}} \mathbf{w}_{m'}^{\mathcal{H}} \mathbf{\Omega}_{w,m} \mathbf{w}_{m'} \right) + 2\mathrm{Re}\{(\mathbf{w}_m^{(p)})^{\mathcal{H}} \mathbf{\Omega}_{w,m} \mathbf{w}_m\} + c_{w,m}, \tag{23}$$

where $c_{w,m} = -(\mathbf{w}_m^{(p)})^{\mathcal{H}} \mathbf{\Omega}_{w,m} \mathbf{w}_m^{(p)} - t_m^* n_m$ is a constant. According to (20) and (22), the UL QoS constraint of (18b) is converted into

$$\left(\sum_{m\in\mathcal{M}} \mathbf{w}_m^{\mathcal{H}} \mathbf{\Omega}_{w,U} \mathbf{w}_m \right) + 2 \left(\sum_{m=1}^{M-1} \sum_{m'=m+1}^{M} 2\mathrm{Re}\{(\mathbf{w}_m^{(p)})^{\mathcal{H}} \mathbf{\Omega}_{w,U} \mathbf{w}_{m'}\} \right) + c_{w,U} \leq 0, \tag{24}$$

where $c_{w,U} = -2 \sum_{m=1}^{M-1} \sum_{m'=m+1}^{M} (\mathbf{w}_m^{(p)})^{\mathcal{H}} \mathbf{\Omega}_{w,U} \mathbf{w}_{m'}^{(p)} - \xi_U$ is a constant. Finally, we have the transformed problem w.r.t. $\mathbf{W}$ as

$$\max_{\mathbf{W}} \ \widetilde{F}_{D,t}(\mathbf{W}) \quad \text{s.t. (11d), (24)}, \tag{25}$$

which is convex and can be solved to obtain the optimal active BS beamforming solution.

2) Optimization of Passive RIS Phase-Shifts: After obtaining the optimal active beamforming solution of $\mathbf{W}^*$, we now consider the subproblem w.r.t. passive beamforming of RIS $\mathbf{\Theta}$. Firstly, we employ a vector

form of RIS phase shift of $\boldsymbol{\theta} = [e^{j\theta_1}, ..., e^{j\theta_k}, ..., e^{j\theta_K}]^{\mathcal{T}} \in \mathbb{C}^K$ instead of matrix form of $\boldsymbol{\Theta}$. Similar to (18), the problem (17) can be reformulated w.r.t. $\boldsymbol{\theta}$ with fixed $\mathbf{W}^*$ as

$$\max_{\boldsymbol{\theta}} \ \widetilde{F}_D^{\theta}(\boldsymbol{\theta}) = \sum_{m\in\mathcal{M}} D_{S,m}(\boldsymbol{\theta}) - t_m^*(D_{t,m}(\boldsymbol{\theta}) + D_{C,m}(\boldsymbol{\theta}) + \sigma^2) \tag{26a}$$

$$\text{s.t. (11c)}, \quad U_S(\boldsymbol{\theta}) - \overline{t}_{th,U}\left(U_I(\boldsymbol{\theta}) + \sigma^2\right) \geq 0, \tag{26b}$$

where pertinent notations w.r.t. $\boldsymbol{\theta}$ are defined as follows.

$$D_{S,m}(\boldsymbol{\theta}) = (1 + r_m^*)\|\mathbf{D}_m\mathbf{w}_m^* + \mathbf{D}_{t_m}\mathbf{w}_m^{*(D)}\boldsymbol{\theta}\|^2, \quad \mathbf{w}_m^{*(D)} = \text{diag}(\mathbf{w}_m^*, \mathbf{w}_m^*, ..., \mathbf{w}_m^*) \in \mathbb{C}^{N\cdot K\times K},$$

$$D_{t,m}(\boldsymbol{\theta}) = \sum_{m'\in\mathcal{M}} \|\mathbf{D}_m\mathbf{w}_{m'}^* + \mathbf{D}_{t_m}\mathbf{w}_{m'}^{*(D)}\boldsymbol{\theta}\|^2, \quad \overline{\mathbf{x}}_U^{(U)} = \text{diag}(\overline{\mathbf{x}}_U, \overline{\mathbf{x}}_U, ..., \overline{\mathbf{x}}_U) \in \mathbb{C}^{NK\times K},$$

$$D_{C,m}(\boldsymbol{\theta}) = \|\mathbf{V}_m\overline{\mathbf{x}}_U + \mathbf{C}_{t_m}\overline{\mathbf{x}}_U^{(U)}\boldsymbol{\theta}\|^2, \quad \mathbf{d}_t^{(D)} = \text{diag}(\mathbf{d}_t, \mathbf{d}_t, ..., \mathbf{d}_t) \in \mathbb{C}^{N_tK\times K}, \ \mathbf{d}_t = \sum_{m\in\mathcal{M}} \mathbf{w}_m^*\overline{x}_{D,m} \in \mathbb{C}^{N_t},$$

$$U_S(\boldsymbol{\theta}) = \|\mathbf{U}\overline{\mathbf{x}}_U + \mathbf{U}_t\overline{\mathbf{x}}_U^{(U)}\boldsymbol{\theta}\|^2, \quad U_I(\boldsymbol{\theta}) = \|\mathbf{S}\mathbf{W}^*\overline{\mathbf{x}}_D + \mathbf{S}_t\mathbf{d}_t^{(D)}\boldsymbol{\theta}\|^2,$$

Therefore, we can have equivalent expressions by moving out the parameter $\boldsymbol{\theta}$ originally within two matrices. Accordingly, by rearranging the above formulas, the objective (26a) can be rewritten in an quadratic form as

$$\widetilde{F}_D(\boldsymbol{\theta}) = \sum_{m\in\mathcal{M}} \boldsymbol{\theta}^{\mathcal{H}}\boldsymbol{\Omega}_{\theta,m}\boldsymbol{\theta} - \boldsymbol{\theta}^{\mathcal{H}}\boldsymbol{\Psi}_{\theta,m}\boldsymbol{\theta} + 2\text{Re}\{\boldsymbol{\zeta}_{\theta,m}\boldsymbol{\theta}\} + c_{\theta,m}, \tag{27}$$

where

$$\boldsymbol{\Omega}_{\theta,m} = (1 + r_m^*)(\mathbf{w}_m^{*(D)})^{\mathcal{H}}\mathbf{D}_{t_m}^{\mathcal{H}}\mathbf{D}_{t_m}\mathbf{w}_m^{*(D)}, \quad \boldsymbol{\Psi}_{\theta,m} = t_m^*\mathbf{D}_{t_m}\sum_{m'\in\mathcal{M}}\left(\mathbf{w}_{m'}^{*(D)}(\mathbf{w}_{m'}^{*(D)})^{\mathcal{H}}\right)\mathbf{D}_{t_m}^{\mathcal{H}},$$

$$\boldsymbol{\zeta}_{\theta,m} = (1 + r_m^*)(\mathbf{w}_m^*)^{\mathcal{H}}\mathbf{D}_m^{\mathcal{H}}\mathbf{D}_{t_m}\mathbf{w}_m^{*(D)} - t_m^*\left(\sum_{m'\in\mathcal{M}}(\mathbf{w}_{m'}^*)^{\mathcal{H}}\mathbf{D}_m^{\mathcal{H}}\mathbf{D}_{t_m}\mathbf{w}_{m'}^{*(D)} + \overline{\mathbf{x}}_U^{\mathcal{H}}\mathbf{V}_m^{\mathcal{H}}\mathbf{C}_{t_m}\overline{\mathbf{x}}_U^{(U)}\right),$$

$$c_{\theta,m} = (1 + r_m^*)(\mathbf{w}_m^*)^{\mathcal{H}}\mathbf{D}_m^{\mathcal{H}}\mathbf{D}_m\mathbf{w}_m^* - t_m^*\left(\sum_{m'\in\mathcal{M}}(\mathbf{w}_{m'}^*)^{\mathcal{H}}\mathbf{D}_m^{\mathcal{H}}\mathbf{D}_m\mathbf{w}_{m'}^* + \overline{\mathbf{x}}_U^{\mathcal{H}}\mathbf{V}_m^{\mathcal{H}}\mathbf{V}_m\overline{\mathbf{x}}_U + \sigma^2\right).$$

Moreover, UL QoS constraint in (26b) can be rewritten in a quadratic form given by

$$\boldsymbol{\theta}^{\mathcal{H}}\boldsymbol{\Omega}_{\theta,U}\boldsymbol{\theta} - \boldsymbol{\theta}^{\mathcal{H}}\boldsymbol{\Psi}_{\theta,U}\boldsymbol{\theta} + 2\text{Re}\{\boldsymbol{\zeta}_{\theta,U}\boldsymbol{\theta}\} + c_{\theta,U} \geq 0, \tag{28}$$

where

$$\boldsymbol{\Omega}_{\theta,U} = (\overline{\mathbf{x}}_U^{(U)})^{\mathcal{H}}\mathbf{U}_t^{\mathcal{H}}\mathbf{U}_t\overline{\mathbf{x}}_U^{(U)}, \quad \boldsymbol{\zeta}_{\theta,U} = \overline{\mathbf{x}}_U^{\mathcal{H}}\mathbf{U}^{\mathcal{H}}\mathbf{U}_t\overline{\mathbf{x}}_U^{(U)} - \overline{t}_{th,U}\overline{\mathbf{x}}_D^{\mathcal{H}}(\mathbf{W}^*)^{\mathcal{H}}\mathbf{S}^{\mathcal{H}}\mathbf{S}_t\mathbf{d}_t^{(D)},$$

$$\boldsymbol{\Psi}_{\theta,U} = \overline{t}_{th,U}(\mathbf{d}_t^{(D)})^{\mathcal{H}}\mathbf{S}_t^{\mathcal{H}}\mathbf{S}_t\mathbf{d}_t^{(D)}, \quad c_{\theta,U} = \overline{\mathbf{x}}_U^{\mathcal{H}}\mathbf{U}^{\mathcal{H}}\mathbf{U}\overline{\mathbf{x}}_U - \overline{t}_{th,U}\left(\overline{\mathbf{x}}_D^{\mathcal{H}}(\mathbf{W}^*)^{\mathcal{H}}\mathbf{S}^{\mathcal{H}}\mathbf{S}\mathbf{W}^*\overline{\mathbf{x}}_D + \sigma^2\right).$$

However, we can observe that (27) and (28) both perform convex-concave functions. Therefore, we employ SCA with the first-order Taylor approximation to transform a non-convex function to affine one, where the inequalities are given by $\boldsymbol{\theta}^{\mathcal{H}}\boldsymbol{\Omega}_{\theta,m}\boldsymbol{\theta} \geq 2\text{Re}\{(\boldsymbol{\theta}^{(q)})^{\mathcal{H}}\boldsymbol{\Omega}_{\theta,m}\boldsymbol{\theta}\} - (\boldsymbol{\theta}^{(q)})^{\mathcal{H}}\boldsymbol{\Omega}_{\theta,m}\boldsymbol{\theta}^{(q)}$ in (27), and $\boldsymbol{\theta}^{\mathcal{H}}\boldsymbol{\Omega}_{\theta,U}\boldsymbol{\theta} \geq 2\text{Re}\{(\boldsymbol{\theta}^{(q)})^{\mathcal{H}}\boldsymbol{\Omega}_{\theta,U}\boldsymbol{\theta}\} - (\boldsymbol{\theta}^{(q)})^{\mathcal{H}}\boldsymbol{\Omega}_{\theta,U}\boldsymbol{\theta}^{(q)}$ in (28), where $\boldsymbol{\theta}^{(q)}$ indicates a constant of RIS solution obtained at the previous iteration q. Accordingly, we can attain an SCA-based objective in (27) as

$$\widetilde{F}_{D,t}(\boldsymbol{\theta}) = \sum_{m\in\mathcal{M}} \boldsymbol{\theta}^{\mathcal{H}}\boldsymbol{\Psi}_{\theta,m}\boldsymbol{\theta} + 2\text{Re}\{\overline{\boldsymbol{\zeta}}_{\theta,m}\boldsymbol{\theta}\} + \overline{c}_{\theta,m}, \tag{29}$$

where $\overline{\boldsymbol{\zeta}}_{\theta,m} = \boldsymbol{\zeta}_{\theta,m} + (\boldsymbol{\theta}^{(q)})^{\mathcal{H}}\boldsymbol{\Omega}_{\theta,m}$ and $\overline{c}_{\theta,m} = c_{\theta,m} - (\boldsymbol{\theta}^{(q)})^{\mathcal{H}}\boldsymbol{\Omega}_{\theta,m}\boldsymbol{\theta}^{(q)}$. Similarly, with SCA, UL QoS constraint of (28) can be expressed as

$$-\boldsymbol{\theta}^{\mathcal{H}}\boldsymbol{\Psi}_{\theta,U}\boldsymbol{\theta} + 2\text{Re}\{\overline{\boldsymbol{\zeta}}_{\theta,U}\boldsymbol{\theta}\} + \overline{c}_{\theta,U} \geq 0, \tag{30}$$

where $\overline{\boldsymbol{\zeta}}_{\theta,U} = (\boldsymbol{\theta}^{(q)})^{\mathcal{H}}\boldsymbol{\Omega}_{\theta,U} + \boldsymbol{\zeta}_{\theta,U}$ and $\overline{c}_{\theta,U} = c_{\theta,U} - (\boldsymbol{\theta}^{(q)})^{\mathcal{H}}\boldsymbol{\Omega}_{\theta,U}\boldsymbol{\theta}^{(q)}$. Accordingly, the problem (26) is transformed as

$$\max_{\boldsymbol{\theta}} \ \widetilde{F}_{D,t}(\boldsymbol{\theta}) \quad \text{s.t. (11c), (30).} \tag{31a}$$

Nevertheless, the equality of RIS phase constraint in (11c) is non-convex. To address this problem, we adopt a CCP procedure, i.e., $|e^{j\theta_k}|^2 = 1$ can be resolved by employing two equivalent inequalities of $|e^{j\theta_k}|^2 \leq 1$ and $|e^{j\theta_k}|^2 \geq 1$. The first inequality is convex due to its circular shape, whilst the second inequality is non-convex. Adopting SCA again for $|e^{j\theta_k}|^2 \geq 1$ yields $2\text{Re}\{(e^{-j\theta_k})^{(q)}e^{j\theta_k}\} - |(e^{j\theta_k})^{(q)}|^2 \geq 1 \Rightarrow \text{Re}\{(e^{-j\theta_k})^{(q)}e^{j\theta_k}\} \geq 1$ since $|(e^{j\theta_k})^{(q)}|^2 = 1$, where $(e^{-j\theta_k})^{(q)}$ indicates the phase solution obtained as a constant at iteration q. However, directly applying these tight constraints may lead to non-convergence or an infeasible problem during iterative optimization. Therefore, PCCP is employed to allow optimization from loose to tight constraints, asymptotically approaching the original equality constraint. The optimization problem w.r.t. RIS configuration of $\boldsymbol{\theta}$ can be expressed as

$$\max_{\boldsymbol{\theta},\mathbf{a},\mathbf{b}} \ \widetilde{F}_{D,t}(\boldsymbol{\theta}) - \lambda^{(q)} \sum_{k\in\mathcal{K}} (a_k + b_k) \tag{32a}$$

$$\text{s.t. (30)}, \quad \left|e^{j\theta_k}\right|^2 \leq 1 + a_k, \quad \forall k \in \mathcal{K}, \tag{32b}$$

$$\text{Re}\{(e^{-j\theta_k})^{(q)}e^{j\theta_k}\} \geq 1 - b_k, \quad \forall k \in \mathcal{K}. \tag{32c}$$

where $\mathbf{a} = [a_1, ..., a_k, .., a_K]^{\mathcal{T}}$ and $\mathbf{b} = [b_1, ..., b_k, ..., b_K]^{\mathcal{T}}$ denote the slake variables imposed on the associated constraints of RIS phase shifts. To this end, we have a convex problem (32), which can be readily resolved by arbitrary convex optimization tools.

The concrete step of the proposed APB scheme is described in Algorithm 1, which includes outer and inner loops. The outer loop aims at computation of Lagrangian dual r_m and Dinkelbach auxiliary parameters

Algorithm 1: Proposed APB Scheme with Perfect CSI

Initialize random active/passive beamforming $\mathbf{W}^{(0)}$ and $\boldsymbol{\theta}^{(0)}$
Set iteration of outer loop $i = 1$
repeat {Outer Loop}
  Compute Lagrangian/Dinkelbach parameters of $r_m^{(i)}$, $t_m^{(i)}$ based on $\mathbf{W}^{(i-1)}$, $\boldsymbol{\theta}^{(i-1)}$
  (BS Active Beamforming):
  Set inner iteration $p = 1$ and $\mathbf{W}_t^{(0)} = \mathbf{W}^{(i-1)}$
  repeat {BS Loop}
    Solve problem (25) for $\mathbf{W}_t^{(p)}$ with fixed $\boldsymbol{\theta}^{(i-1)}$
    Update $p \leftarrow p + 1$
  until Convergence of $\mathbf{W}_t$
  Obtain $\mathbf{W}_t^* = \mathbf{W}_t^{(p-1)}$
  (RIS Passive Beamforming):
  Set inner iteration $q = 1$ and $\boldsymbol{\theta}_t^{(0)} = \boldsymbol{\theta}^{(i-1)}$, $\kappa \geq 0$, $\lambda^{(0)} = 1$ and $\lambda_{\max}$
  repeat {RIS Loop}
    Solve problem (32) for $\boldsymbol{\theta}_t^{(q)}$ with fixed $\mathbf{W}_t^*$
    Update $\lambda^{(q)} = \min\left\{\kappa\lambda^{(q-1)}, \lambda_{\max}\right\}$.
    Update $q \leftarrow q + 1$
  until Convergence of $\boldsymbol{\theta}_t$
  Obtain $\boldsymbol{\theta}_t^* = \boldsymbol{\theta}_t^{(q-1)}$ and $\left\{\boldsymbol{\theta}^{(i)}, \mathbf{W}^{(i)}\right\} = \{\boldsymbol{\theta}_t^*, \mathbf{W}_t^*\}$
  Update $i \leftarrow i + 1$
until Convergence of total solution
return $\{\boldsymbol{\theta}^*, \mathbf{W}^*\} = \left\{\boldsymbol{\theta}^{(i-1)}, \mathbf{W}^{(i-1)}\right\}$.

of t_m. With the benefit of AO algorithm, the inner loop consists of active and passive beamforming, resolving problems (25) and (32), respectively. We notice the problem (32) is solved using the most recent result from (25) at current iteration. It is important to mention that the update of RIS penalty terms will be performed after obtaining the temporary candidate solution of RIS beamforming. The whole procedure will be iteratively executed until their respective convergence given by

$$|\widetilde{F}_{D,t}^{(p)}(\mathbf{W}) - \widetilde{F}_{D,t}^{(p-1)}(\mathbf{W})| \leq \varrho_w, \quad |\widetilde{F}_{D,t}^{(q)}(\boldsymbol{\theta}) - \widetilde{F}_{D,t}^{(q-1)}(\boldsymbol{\theta})| \leq \varrho_\theta, \quad |\widetilde{F}_{D}^{(i)}(\boldsymbol{\Theta}, \mathbf{W}) - \widetilde{F}_{D}^{(i-1)}(\boldsymbol{\Theta}, \mathbf{W})| \leq \varrho, \quad (33)$$

where ϱ_w, ϱ_θ, and ϱ indicate the respective convergence bounds. To elaborate a little further, we select the historical optimal solution if the iteration exceeds their respective upper bounds, i.e., $p > T_w$, $q > T_\theta$, and $i > T$.

IV. Proposed RAPB Scheme with Imperfect CSI

A. Problem Transformation for Robustness

In the case of imperfect CSI, we consider $\triangle\mathbf{D}_{t_m} \neq 0$, $\triangle\mathbf{C}_{t_m} \neq$, $\triangle\mathbf{U}_t \neq 0$, and $\triangle\mathbf{S}_t \neq 0$. We consider the imperfect CSI of the reflected channels from BS to RIS and from RIS to UEs w.r.t. their first and second

moments in (6) and (7). According to distirbutionally robust optimization, we firstly reformulate the original problem (11) as the equivalent one as

$$\max_{\boldsymbol{\Theta},\mathbf{W},\boldsymbol{\gamma}_D} \sum_{m\in\mathcal{M}} \gamma_{D,m} \tag{34a}$$

$$\text{s.t.} \inf_{\mathfrak{D}\in\mathcal{P}} \mathbb{P}_{\mathfrak{D}}\{\log_2(1+\text{SINR}_{D,m}^{r}) \geq \gamma_{D,m}\} \geq 1-\epsilon_m, \quad \forall m \in \mathcal{M}, \tag{34b}$$

$$\inf_{\mathfrak{D}\in\mathcal{P}} \mathbb{P}_{\mathfrak{D}}\{\log_2(1+\text{SINR}_{U}^{r}) \geq \gamma_{U}\} \geq 1-\epsilon_U, \tag{34c}$$

$$\mathcal{P} = \{\mathfrak{D} : (6), (7)\}. \tag{34d}$$

$$(11c), (11d). \tag{34e}$$

In the robust problem of (34), $\gamma_{D,m} \in \boldsymbol{\gamma}_D$ in (34a) and (34b) indicates the lower bound of total DL rate. That is, the original problem of DL rate-maximization is guaranteed if the lower bound of $\gamma_{D,m}$ is maximized. The chance constraints of (34b) and (34c) imply that the minimum probability of DL/UL rate higher than $\gamma_{D,m}$ should be greater than $1-\epsilon_m$ and $1-\epsilon_U$, where $0 \leq \epsilon_m \leq 1$ and $0 \leq \epsilon_U \leq 1$ denote the threshold of outage probability for DL and UL rates, respectively. That is, the worst case of SINR satisfaction should be satisfied above the certain thresholds. Moreover, $\mathbb{P}_{\mathfrak{D}}$ indicates the probability under the distribution of $\mathfrak{D}$, where $\mathfrak{D} \in \mathcal{P}$ in the constraint of (34d) comprises imperfect CSI information. Note that the existence of probability is because of the stochastic expression of SINR induced by channel errors. Similar to (12b), in (34c), we consider Jensen's inequality for the lower bound of total UL rate bound for further derivation. For the problem (34), there exist no closed-forms in (34b) and (34c) because of their probability expressions. Moreover, the coupled variables in active and passive beamforming lead to an unsolvable problem. We employ AO algorithm to decouple the original problem into two sub-problems w.r.t. active and passive beamforming optimization. In the following respective sub-problems, we focus on tackling the DL/UL outage probability constraints. The overall procedure of RAPB problem is illustrated in Fig. 3.

B. Optimization of Active Beamforming with Imperfect CSI

With fixed RIS phase matrix $\boldsymbol{\Theta}^*$, the original problem (34) is reduced to

$$\max_{\mathbf{W},\boldsymbol{\gamma}_D} \sum_{m\in\mathcal{M}} \gamma_{D,m} \tag{35a}$$

$$\text{s.t.} \inf_{\mathfrak{D}\in\mathcal{P}} \mathbb{P}_{\mathfrak{D}}\{\log_2(1+\text{SINR}_{D,m}^{r,w}) \geq \gamma_{D,m}\} \geq 1-\epsilon_m, \quad \forall m \in \mathcal{M}, \tag{35b}$$

$$\inf_{\mathfrak{D}\in\mathcal{P}} \mathbb{P}_{\mathfrak{D}}\{\log_2(1+\text{SINR}_{U}^{r,w}) \geq \gamma_{U}\} \geq 1-\epsilon_U, \tag{35c}$$

$$(11d), (34d), \tag{35d}$$

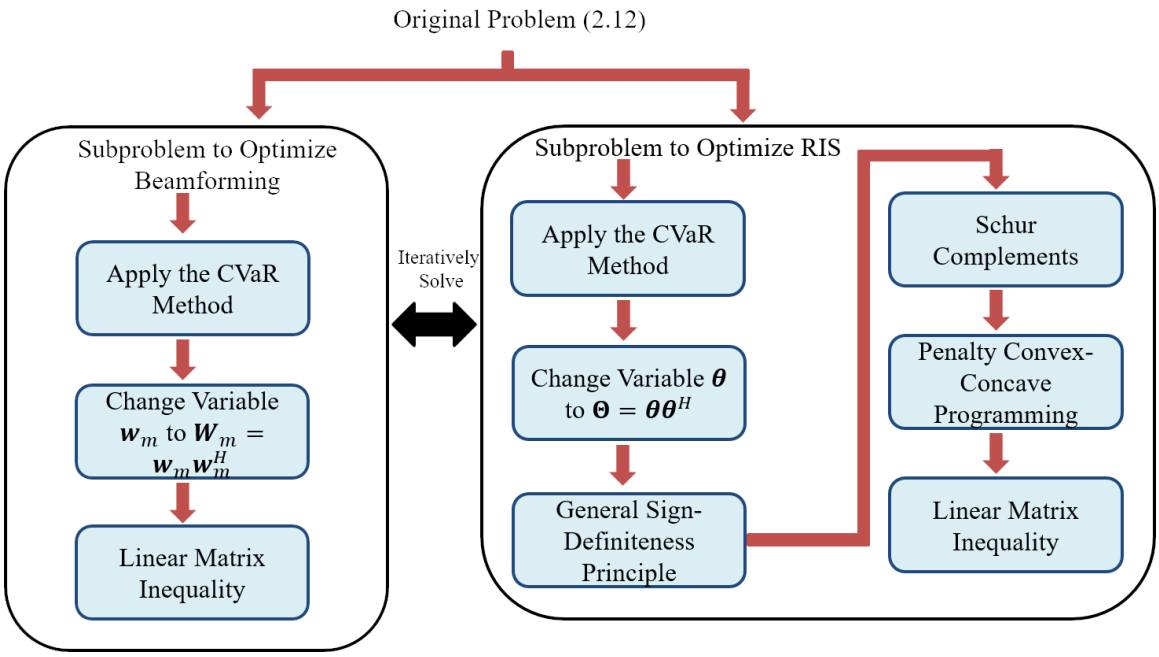

Fig. 3. Flowchart of robust problem transformation.

where $\text{SINR}_{D,m}^{r,w} = \frac{\|(\mathbf{D}_m+(\widetilde{\mathbf{D}}_{t_m}+\triangle\mathbf{D}_{t_m})\boldsymbol{\Theta}^{*(D)})\mathbf{w}_m\overline{\mathbf{x}}_{D,m}\|^2}{\sum_{m'\in\mathcal{M}\setminus m}\|(\mathbf{D}_m+(\widetilde{\mathbf{D}}_{t_m}+\triangle\mathbf{D}_{t_m})\boldsymbol{\Theta}^{*(D)})\mathbf{w}_{m'}\overline{x}_{D,m'}\|^2+\|(\mathbf{V}_m+(\widetilde{\mathbf{C}}_{t_m}+\triangle\mathbf{C}_{t_m})\boldsymbol{\Theta}^{*(D)})\overline{\mathbf{x}}_U\|^2+\sigma^2}$ and $\text{SINR}_U^{r,w} = \frac{\|(\mathbf{U}+(\widetilde{\mathbf{U}}_t+\triangle\mathbf{U}_t)\boldsymbol{\Theta}^{*(U)})\overline{\mathbf{x}}_U\|^2}{\|\sqrt{p_D}(\mathbf{S}+(\widetilde{\mathbf{S}}_t+\triangle\mathbf{S}_t)\boldsymbol{\Theta}^{*(U)})\mathbf{W}\overline{\mathbf{x}}_D\|^2+\sigma^2}$ are SINR parameters with fixed optimal RIS configuration $\boldsymbol{\Theta}^*$. First, we deal with the term inside probability of the DL chance constraint (35b) as

$$\text{SINR}_{D,m}^{r,w} \geq \overline{\gamma}_{D,m} \quad \Rightarrow \frac{p_D\|\mathbf{D}_m\mathbf{w}_m + \hat{\mathbf{D}}_{t_m}\mathbf{w}_m\|^2}{\sum_{m'\in\mathcal{M}\setminus m} p_D\|\mathbf{D}_m\mathbf{w}_{m'} + \hat{\mathbf{D}}_{t_m}\mathbf{w}_{m'}\|^2+\|\mathbf{V}_m\overline{\mathbf{x}}_U + \hat{\mathbf{C}}_{t_m}\overline{\mathbf{x}}_U\|^2+\sigma^2} \geq \overline{\gamma}_{D,m}, \tag{36}$$

where $\hat{\mathbf{D}}_{t_m} = (\widetilde{\mathbf{D}}_{t_m} + \triangle\mathbf{D}_{t_m})\boldsymbol{\Theta}^{*(D)}$, $\hat{\mathbf{C}}_{t_m} = (\widetilde{\mathbf{C}}_{t_m} + \triangle\mathbf{C}_{t_m})\boldsymbol{\Theta}^{*(D)}$, and $\overline{\gamma}_{D,m} = 2^{\gamma_{D,m}} - 1$. As a result, the objective for this subproblem is alternated from $\gamma_{D,m}$ to $\overline{\gamma}_{D,m}$. Then, we define $\mathbf{t}_{r_{w,m}} \in \mathbb{R}^{1\times(2N_t+2N)}$ as the imperfect CSI for DL SINR as

$$\mathbf{t}_{r_{w,m}} = \left[\text{Re}\{\hat{\mathbf{D}}_{t_m}\}, \text{Im}\{\hat{\mathbf{D}}_{t_m}\}, \text{Re}\{\hat{\mathbf{C}}_{t_m}\}, \text{Im}\{\hat{\mathbf{C}}_{t_m}\}\right]. \tag{37}$$

Assume that $f_{w,m} : \mathbb{R}^{1\times(2N_t+2N)} \to \mathbb{R}$ and (36) can be reformulated in a quadratic form given by

$$f_{w,m}(\mathbf{t}_{r_{w,m}}) \geq 0 \Rightarrow \mathbf{t}_{r_{w,m}}\mathbf{Q}_{w,m}(\mathbf{W})\mathbf{t}_{r_{w,m}}^{\mathcal{T}} + 2\mathbf{q}_{w,m}(\mathbf{W})\mathbf{t}_{r_{w,m}}^{\mathcal{T}} + q_{w,m}^0(\mathbf{W}) \geq 0, \tag{38}$$

where

$$\mathbf{Q}_{w,m}(\mathbf{W}) = \begin{bmatrix} \mathrm{Re}\{\boldsymbol{\Upsilon}_{w,m}\} & \mathrm{Im}\{\boldsymbol{\Upsilon}_{w,m}\} & \mathbf{0} & \mathbf{0} \\ -\mathrm{Im}\{\boldsymbol{\Upsilon}_{w,m}\} & \mathrm{Re}\{\boldsymbol{\Upsilon}_{w,m}\} & \mathbf{0} & \mathbf{0} \\ \mathbf{0} & \mathbf{0} & \mathrm{Re}\{\boldsymbol{\Upsilon}_{w,V_m}\} & \mathrm{Im}\{\boldsymbol{\Upsilon}_{w,V_m}\} \\ \mathbf{0} & \mathbf{0} & -\mathrm{Im}\{\boldsymbol{\Upsilon}_{w,V_m}\} & \mathrm{Re}\{\boldsymbol{\Upsilon}_{w,V_m}\} \end{bmatrix} \in \mathbb{R}^{(2N_t+2N)\times(2N_t+2N)},$$

$$\mathbf{q}_{w,m}(\mathbf{W}) = \left[\mathrm{Re}\left\{\boldsymbol{\Xi}_{w,m}\right\}, \mathrm{Im}\left\{\boldsymbol{\Xi}_{w,m}\right\}, \mathrm{Re}\left\{\boldsymbol{\Xi}_{w,V_m}\right\}, \mathrm{Im}\left\{\boldsymbol{\Xi}_{w,V_m}\right\}\right] \in \mathbb{R}^{1\times(2N_t+2N)}, \tag{39}$$

$$q^0_{w,m}(\mathbf{W}) = p_D \mathbf{w}_m^{\mathcal{H}} \mathbf{D}_m^{\mathcal{H}} \mathbf{D}_m \mathbf{w}_m - \overline{\gamma}_{D,m} \left(\sum_{m' \in \mathcal{M}\setminus m} p_D \mathbf{w}_{m'}^{\mathcal{H}} \mathbf{D}_m^{\mathcal{H}} \mathbf{D}_m \mathbf{w}_{m'} + \overline{\mathbf{x}}_U^{\mathcal{H}} \mathbf{V}_m^{\mathcal{H}} \mathbf{V}_m \overline{\mathbf{x}}_U + \sigma^2 \right) \in \mathbb{R},$$

where $\boldsymbol{\Upsilon}_{w,m} = p_D \mathbf{w}_m \mathbf{w}_m^{\mathcal{H}} - \overline{\gamma}_{D,m} \sum_{m' \in \mathcal{M}\setminus m} \mathbf{w}_{m'} \mathbf{w}_{m'}^{\mathcal{H}}$, $\boldsymbol{\Upsilon}_{w,V_m} = \overline{\mathbf{x}}_U \overline{\mathbf{x}}_U^{\mathcal{H}}$, $\boldsymbol{\Xi}_{w,m} = p_D \mathbf{D}_m \mathbf{w}_m \mathbf{w}_m^{\mathcal{H}}$, and $\boldsymbol{\Xi}_{w,V_m} = \mathbf{V}_m \overline{\mathbf{x}}_U \overline{\mathbf{x}}_U^{\mathcal{H}}$. Therefore, the alternative DL chance constraint (35b) can be rewritten as

$$\inf_{\mathfrak{D}\in\mathcal{P}} \mathbb{P}_{\mathfrak{D}}\{f_{w,m}(\mathbf{t}_{r_{w,m}}) \geq 0\} \geq 1 - \epsilon_m, \quad \forall m \in \mathcal{M}. \tag{40}$$

In a similar way, we reconstruct alternative expression of UL QoS chance constraint of (35c) as

$$\mathrm{SINR}_U^{r,w} \geq \overline{\gamma}_U \Rightarrow \frac{\|\mathbf{U}\overline{\mathbf{x}}_U + \mathbf{U}_t \boldsymbol{\Theta}^{*(U)} \overline{\mathbf{x}}_U\|^2}{\|\mathbf{S}\mathbf{W}\overline{\mathbf{x}}_D + \mathbf{S}_t \boldsymbol{\Theta}^{*(U)} \mathbf{W}\overline{\mathbf{x}}_D\|^2 + \sigma^2} \geq \overline{\gamma}_U \Rightarrow \frac{\|\mathbf{U}\overline{\mathbf{x}}_U + \hat{\mathbf{U}}_t\|^2}{\|\mathbf{S}\mathbf{W}\overline{\mathbf{x}}_D + \mathbf{W}'\hat{\mathbf{S}}_t\|^2 + \sigma^2} \geq \overline{\gamma}_U, \tag{41}$$

where $\overline{\gamma}_U = 2^{\gamma_U} - 1$, $\hat{\mathbf{U}}_t = \mathbf{U}_t \boldsymbol{\Theta}^{*(U)} \overline{\mathbf{x}}_U \in \mathbb{C}^{N_r}$, $\mathbf{W}' = \sum_{m\in\mathcal{M}} [\mathbf{E}_{1,m}, ..., \mathbf{E}_{n_t,m}, ..., \mathbf{E}_{N_t,m}] \in \mathbb{C}^{N_r \times N_r N_t}$, $\mathbf{E}_{n_t,m} = w_{n_t,m} \mathbf{I}_{N_r} \in \mathbb{C}^{N_r \times N_r}, \forall m \in \mathcal{M}, n_t \in \mathcal{N}_t$, $\hat{\mathbf{S}}_\theta = \mathbf{S}_t \boldsymbol{\Theta}^{*(U)} \in \mathbb{C}^{N_r \times N_t}$, and $\hat{\mathbf{S}}_t = [\hat{S}_{\theta_{1,1}}, ..., \hat{S}_{\theta_{N_r,1}}, \hat{S}_{\theta_{1,2}}, ..., \hat{S}_{\theta_{N_r,2}}, ..., \hat{S}_{\theta_{1,N_t}}, ..., \hat{S}_{\theta_{N_r,N_t}}]^{\mathcal{T}} \in \mathbb{C}^{N_r N_t}$. Note that $\hat{S}_{\theta_{n_r,n_t}}$ is the element in the column n_r and row n_t of $\hat{\mathbf{S}}_\theta$. Notation $w_{n_t,m}$ is the element in the column n_t and row m of $\mathbf{W}$. Then, we define $\mathbf{t}_{r_{w,U}} \in \mathbb{R}^{1\times(2N_r+2N_rN_t)}$ as the imperfect CSI for UL SINR as

$$\mathbf{t}_{r_{w,U}} = \left[\mathrm{Re}\{\hat{\mathbf{U}}_t\}, \mathrm{Im}\{\hat{\mathbf{U}}_t\}, \mathrm{Re}\{\hat{\mathbf{S}}_t\}, \mathrm{Im}\{\hat{\mathbf{S}}_t\}\right]. \tag{42}$$

Assume that $f_{w,U} : \mathbb{R}^{1\times(2N_r+2N_rN_t)} \to \mathbb{R}$ and the equation of (41) can be reformulated as

$$f_{w,U}(\mathbf{t}_{r_{w,U}}) \geq 0 \Rightarrow \mathbf{t}_{r_{w,U}} \mathbf{Q}_{w,U}(\mathbf{W}) \mathbf{t}_{r_{w,U}}^{\mathcal{T}} + 2\mathbf{q}_{w,U}(\mathbf{W}) \mathbf{t}_{r_{\theta,U}}^{\mathcal{T}} + q^0_{w,U} \geq 0, \tag{43}$$

where

$$\begin{aligned} \mathbf{Q}_{w,U}(\mathbf{W}) &= \begin{bmatrix} \mathrm{Re}\{\boldsymbol{\Upsilon}_{w,C}\} & \mathrm{Im}\{\boldsymbol{\Upsilon}_{w,C}\} & \mathbf{0} & \mathbf{0} \\ -\mathrm{Im}\{\boldsymbol{\Upsilon}_{w,C}\} & \mathrm{Re}\{\boldsymbol{\Upsilon}_{w,C}\} & \mathbf{0} & \mathbf{0} \\ \mathbf{0} & \mathbf{0} & \mathrm{Re}\{\boldsymbol{\Upsilon}_{w,S}\} & \mathrm{Im}\{\boldsymbol{\Upsilon}_{w,S}\} \\ \mathbf{0} & \mathbf{0} & -\mathrm{Im}\{\boldsymbol{\Upsilon}_{w,S}\} & \mathrm{Re}\{\boldsymbol{\Upsilon}_{w,S}\} \end{bmatrix} \in \mathbb{R}^{(2N_r+2N_rN_t)\times(2N_r+2N_rN_t)} \\ \mathbf{q}_{w,U}(\mathbf{W}) &= [\mathrm{Re}\{\boldsymbol{\Xi}_{w,C}\}, \mathrm{Im}\{\boldsymbol{\Xi}_{w,C}\}, \mathrm{Re}\{\boldsymbol{\Xi}_{w,S}\}, \mathrm{Im}\{\boldsymbol{\Xi}_{w,S}\}], \in \mathbb{R}^{1\times(2N_r+2N_rN_t)} \\ q^0_{w,U}(\mathbf{W}) &= \overline{\mathbf{x}}_U^{\mathcal{H}} \mathbf{U}^{\mathcal{H}} \mathbf{U} \overline{\mathbf{x}}_U - \overline{\gamma}_U \left(\overline{\mathbf{x}}_D^{\mathcal{H}} \mathbf{W}^{\mathcal{H}} \mathbf{S}^{\mathcal{H}} \mathbf{S} \mathbf{W} \overline{\mathbf{x}}_D + \sigma^2 \right) \\ &= \overline{\mathbf{x}}_U^{\mathcal{H}} \mathbf{U}^{\mathcal{H}} \mathbf{U} \overline{\mathbf{x}}_U - \overline{\gamma}_U \left(p_D \sum_{m\in\mathcal{M}} \mathbf{w}_m^{\mathcal{H}} \mathbf{S}^{\mathcal{H}} \mathbf{S} \sum_{m\in\mathcal{M}} \mathbf{w}_m + \sigma^2 \right) \in \mathbb{R}, \end{aligned} \tag{44}$$

where the pertinent parameters in $\mathbf{Q}_{w,U}(\mathbf{W})$, $\mathbf{q}_{w,U}(\mathbf{W})$, and $q^0_{w,U}$ are defined as follows.

$$\boldsymbol{\Upsilon}_{w,C} = \mathbf{I}_{N_r}, \quad \boldsymbol{\Xi}_{w,C} = \overline{\mathbf{x}}_U^{\mathcal{H}} \mathbf{U}^{\mathcal{H}}, \quad \boldsymbol{\Xi}_{w,S} = -\overline{\gamma}_U \hat{\mathbf{S}}_t \left(\sum_{m \in \mathcal{M}} \left(\mathbf{w}_m \mathbf{w}_m^{\mathcal{H}} \right)^{\dagger} \otimes \mathbf{I}_{N_r} + \sum_{n=1}^{M-1} \sum_{m'=n+1}^{M} \mathbf{w}_n \mathbf{w}_{m'}^{\mathcal{H}} \otimes \mathbf{I}_{N_r} \right),$$

$$\begin{aligned}
\boldsymbol{\Upsilon}_{w,S} &= -\overline{\gamma}_U \mathbf{W}'^{\mathcal{H}} \mathbf{W}' \\
&= -\overline{\gamma}_U \sum_{m \in \mathcal{M}} \begin{bmatrix} w_{m,1} w_{m,1}^{\mathcal{H}} \cdot \mathbf{I}_{N_r} & \cdots & w_{m,N_t} w_{m,1}^{\mathcal{H}} \cdot \mathbf{I}_{N_r} \\ \vdots & \ddots & \vdots \\ w_{m,1} w_{m,N_t}^{\mathcal{H}} \cdot \mathbf{I}_{N_r} & \cdots & w_{m,N_t} w_{m,N_t}^{\mathcal{H}} \cdot \mathbf{I}_{N_r} \end{bmatrix} - \overline{\gamma}_U \sum_{n=1}^{M-1} \sum_{m'=n+1}^{M} \begin{bmatrix} w_{n,1} w_{m',1}^{\mathcal{H}} \cdot \mathbf{I}_{N_r} & \cdots & w_{n,N_t} w_{m',1}^{\mathcal{H}} \cdot \mathbf{I}_{N_r} \\ \vdots & \ddots & \vdots \\ w_{n,1} w_{m',N_t}^{\mathcal{H}} \cdot \mathbf{I}_{N_r} & \cdots & w_{n,N_t} w_{m',N_t}^{\mathcal{H}} \cdot \mathbf{I}_{N_r} \end{bmatrix} \\
&= -\overline{\gamma}_U \sum_{m \in \mathcal{M}} \left(\mathbf{w}_m \mathbf{w}_m^{\mathcal{H}} \right)^{\dagger} \otimes \mathbf{I}_{N_r} - \overline{\gamma}_U \sum_{n=1}^{M-1} \sum_{m'=n+1}^{M} \mathbf{w}_n \mathbf{w}_{m'}^{\mathcal{H}} \otimes \mathbf{I}_{N_r},
\end{aligned}$$

where † indicates the conjugate operation and $\otimes$ denotes the Kronecker product. Therefore, the UL QoS chance constraint (35c) can be rewritten as

$$\inf_{\mathfrak{D} \in \mathcal{P}} \mathbb{P}_{\mathfrak{D}} \{ f_{w,U}(\mathbf{t}_{r_{w,U}}) \geq 0 \} \geq 1 - \epsilon_U. \tag{45}$$

Originally, value-at-risk is a statistical measure commonly applied in risk management to quantify the potential loss of an investment at a given confidence level, i.e., the maximum expected loss that may take place with a probability within a defined frame. While, CVaR provides additional information about the tail risk beyond VaR [39], which considers not only the probability of an extreme event but also the magnitude of loss when that event occurs. In this sense, in our problem, the value of CVaR has asymptotic meaning of outage, i.e., the estimate of SINR probability that may not be satisfied, which is regarded as the tightest convex approximation of the chance constraint. Based on [40], we can transform the chance constraints of (40) and (45) into CVaR constraints as follows.

Lemma 1. *The transformed chance constraints of DL SINR in* (40) *and UL SINR in* (45) *are equivalent to CVaR expressions as*

$$\inf_{\mathfrak{D} \in \mathcal{P}} \mathbb{P}_{\mathfrak{D}} \{ f_{w,x}(\mathbf{t}_{r_{w,x}}) \geq 0 \} \geq 1 - \epsilon_x \Leftrightarrow \sup_{\mathfrak{D} \in \mathcal{P}} \mathfrak{D}\text{-CVaR}_{\epsilon_x} \left(\hat{f}_{w,x}(\mathbf{t}_{r_{w,x}}) \right) \leq 0, \tag{46}$$

where $x \in \{m, U\}$ indicates the index of DL or representation for UL. Also, we define $\hat{f}_{w,x}(\mathbf{t}_{r_{w,x}}) = -f_{w,x}(\mathbf{t}_{r_{w,x}})$. The inequality at right-hand side indicates the maximum conditional risk values lower than zero, which is defined as [41]

$$\mathfrak{D}\text{-CVaR}_{\epsilon_x} \left(\hat{f}_{w,x}(\mathbf{t}_{r_{w,x}}) \right) = \inf_{\nu_{w,x} \in \mathbb{R}} \left\{ \nu_{w,x} + \frac{1}{\epsilon_x} \mathbb{E}_{\mathfrak{D}} \{ (\hat{f}_{w,x}(\mathbf{t}_{r_{w,x}}) - \nu_{w,x})^+ \} \right\}, \tag{47}$$

Note that $\nu_{w,x}$ denotes the risk threshold and $(x)^+ = \max\{0, x\}$.

Proof. From the left-hand side of (46), we consider the worst-case value-at-risk of the DL SINR constraint $f_{w,x}(\mathbf{t}_{r_{w,x}})$ as

$$\text{WC-VaR}_{\epsilon_x}\left(\hat{f}_{w,x}(\mathbf{t}_{r_{w,x}})\right) = \inf_{\gamma\in\mathbb{R}}\left\{\gamma : \inf_{\mathfrak{D}\in\mathcal{P}} \mathbb{P}_{\mathfrak{D}}\{\hat{f}_{w,x}(\mathbf{t}_{r_{w,x}}) \le \gamma\} \ge 1-\epsilon_x\right\}. \tag{48}$$

Note that (48) indicates the equivalence to the $(1-\epsilon_x)$-quantile of function $\hat{f}_{w,x}(\mathbf{t}_{r_{w,x}})$ under the worst-case distribution of $\mathfrak{D}$. Based on definition, we know that the minimum value of probability w.r.t. negative $\hat{f}_{w,x}(\mathbf{t}_{r_{w,x}})$ represents the value of the worst case which should be smaller than zero. Therefore, we can readily show the following equivalence given by

$$\inf_{\mathfrak{D}\in\mathcal{P}} \mathbb{P}_{\mathfrak{D}}\{\hat{f}_{w,x}(\mathbf{t}_{r_{w,x}}) \le 0\} \ge 1-\epsilon_x \Leftrightarrow \text{WC-VaR}_{\epsilon_x}\left(\hat{f}_{w,x}(\mathbf{t}_{r_{w,x}})\right) \le 0. \tag{49}$$

If the left-hand side of (49) is satisfied, then we can have the solution of $\gamma = 0$ in (48). Moreover, we can know that the maximum risk value should be the worst-case one, i.e.,

$$\sup_{\mathfrak{D}\in\mathcal{P}} \mathfrak{D}\text{-CVaR}_{\epsilon_x}\left(\hat{f}_{w,x}(\mathbf{t}_{r_{w,x}})\right) \Leftrightarrow \text{WC-VaR}_{\epsilon_x}\left(\hat{f}_{w,x}(\mathbf{t}_{r_{w,x}})\right). \tag{50}$$

Therefore, we can derive (46) for both DL/UL constraints by comparing (49) and (50). This completes the proof. □

However, after transformation from Lemma 1, the DL/UL chance constraints in CVaR forms are still non-solvable. Note that the following proposition employs semidefinite programming (SDP) alternative for the worst-case CVaR, which aims for transforming CVaR constraints into closed-forms.

Proposition 2. *The feasible set of* $\mathbf{W}$ *in DL/UL chance constraints of* (46) *given by*

$$\left\{\mathbf{W}\in\mathbb{C}^{N_t\times M} : \sup_{\mathfrak{D}\in\mathcal{P}} \mathfrak{D}\text{-CVaR}_{\epsilon_x}\left(\hat{f}_{w,x}(\mathbf{t}_{r_{w,x}})\right) \le 0, \forall x\in\{m,U\}\right\}, \tag{51}$$

is equivalent to

$$\left\{\begin{array}{l} \mathbf{M}_{w,x}\succeq 0, \nu_{w,x} + \dfrac{1}{\epsilon_x}\text{Tr}\left(\mathbf{\Omega}_{w,x}\mathbf{M}_{w,x}\right) \le 0, \\ \mathbf{M}_{w,x} - \begin{bmatrix} \hat{\mathbf{Q}}_{w,x}(\mathbf{W}) & \frac{\hat{\mathbf{q}}_{w,x}(\mathbf{W})^{\mathcal{T}}}{2} \\ \frac{\hat{\mathbf{q}}_{w,x}(\mathbf{W})}{2} & \hat{q}^0_{w,x}(\mathbf{W}) - \nu_{w,x} \end{bmatrix} \succeq 0. \end{array}\right\}, \tag{52}$$

where $\text{Tr}(\cdot)$ *is the trace operation of a matrix. We denote* $\hat{\mathbf{Q}}_{w,x}(\mathbf{W}) = -\mathbf{Q}_{w,x}(\mathbf{W})$, $\hat{\mathbf{q}}_{w,x}(\mathbf{W}) = -\mathbf{q}_{w,x}(\mathbf{W})$, *and* $\hat{q}^0_{w,x}(\mathbf{W}) = -q^0_{w,x}(\mathbf{W})$, $\forall x\in\{m,U\}$. *The dimensions for DL parameters are* $\nu_{w,m}\in\mathbb{R}$ *and* $\mathbf{M}_{w,m}\in\mathbb{R}_{\mathbb{S}}^{(2N_t+2N+1)}$, *whilst the dimensions for UL ones are* $\nu_{w,U}\in\mathbb{R}$ *and* $\mathbf{M}_{w,U}\in\mathbb{R}_{\mathbb{S}}^{(2N_r+2N_rN_t+1)}$. *Note that* $\mathbf{M}_{w,m}$ *and* $\mathbf{M}_{w,U}$ *are symmetric matrices, whilst* $\mathbb{R}_{\mathbb{S}}$ *stands for the domain of a symmetric matrix. Let the*

second-order moment matrix of $\mathbf{t}_{r_{w,x}}$ *is*

$$\mathbf{\Omega}_{w,x} = \begin{bmatrix} \delta\mathbf{\Sigma}_{w,x} + \boldsymbol{\mu}_{w,x}\boldsymbol{\mu}_{w,x}^{\mathcal{T}} & \boldsymbol{\mu}_{w,x} \\ \boldsymbol{\mu}_{w,x}^{\mathcal{T}} & 1 \end{bmatrix}, \tag{53}$$

where $\mathbb{E}_{\mathfrak{D}}\{\left(\mathbf{t}_{r_{w,x}} - \boldsymbol{\mu}_{w,x}\right)\left(\mathbf{t}_{r_{w,x}} - \boldsymbol{\mu}_{w,x}\right)^{\mathcal{T}}\} = \delta\mathbf{\Sigma}_{w,x}$ *and* $\mathbb{E}_{\mathfrak{D}}\{\mathbf{t}_{r_{w,x}}\} = \boldsymbol{\mu}_{w,x}$ *indicate the covariance and mean of* $\mathbf{t}_{r_{w,x}}$*, which are respectively complied with the original definitions in* (6) *and* (7) *as well as constraint of* (34d).

Proof. Based on (47) in Lemma 1, the worst-case CVaR in (46) can be alternatively expressed as

$$\begin{aligned} \sup_{\mathfrak{D}\in\mathcal{P}} \mathfrak{D}\text{-CVaR}_{\epsilon_x}\left(\hat{f}_{w,x}(\mathbf{t}_{r_{w,x}})\right) &= \sup_{\mathfrak{D}\in\mathcal{P}} \inf_{\nu_{w,x}\in\mathbb{R}} \left\{\nu_{w,x} + \frac{1}{\epsilon_x}\mathbb{E}_{\mathfrak{D}}\{(\hat{f}_{w,x}(\mathbf{t}_{r_{w,x}}) - \nu_{w,x})^{+}\}\right\} \\ &= \inf_{\nu_{w,x}\in\mathbb{R}} \left\{\nu_{w,x} + \frac{1}{\epsilon_x}\sup_{\mathfrak{D}\in\mathcal{P}} \mathbb{E}_{\mathfrak{D}}\{(\hat{f}_{w,x}(\mathbf{t}_{r_{w,x}}) - \nu_{w,x})^{+}\}\right\}, \end{aligned} \tag{54}$$

where operational interchange between $\sup$ and $\inf$ is proved by stochastic saddle point in [42]. In this context, we can reformulate an SDP problem of $\sup_{\mathfrak{D}\in\mathcal{P}} \mathbb{E}_{\mathfrak{D}}\{(\hat{f}_{w,x}(\mathbf{t}_{r_{w,x}}) - \nu_{w,x})^{+}\}$. Therefore, the expectation of the worst-case can be equivalently expressed as

$$\begin{aligned} \varpi_{w,x} = \sup_{\varsigma\in\mathcal{M}^{+}} & \int \varsigma \max\left\{0, \hat{f}_{w,x}(\mathbf{t}_{r_{w,x}}) - \nu_{w,x}\right\} d\mathbf{t}_{r_{w,x}} \\ \text{s.t.} & \int \varsigma d\mathbf{t}_{r_{w,x}} = 1, \quad \int \mathbf{t}_{r_{w,x}}\varsigma d\mathbf{t}_{r_{w,x}} = \boldsymbol{\mu}_{w,x}, \quad \int \mathbf{t}_{r_{w,x}}\mathbf{t}_{r_{w,x}}^{\mathcal{T}}\varsigma d\mathbf{t}_{r_{w,x}} = \mathbf{\Sigma}_{w,x} + \boldsymbol{\mu}_{w,x}\boldsymbol{\mu}_{w,x}^{\mathcal{T}}, \end{aligned} \tag{55}$$

where $\mathcal{M}^{+}$ represents the cone of non-negative measures on the dimension of $\mathbf{t}_{r_{w,x}}$. According to (55), we can have the following dual problem

$$\inf \ A_{w,x} \triangleq m_{w,x}^{0} + \mathbf{m}_{w,x}^{\mathcal{T}}\boldsymbol{\mu}_{w,x} + \text{Tr}\left(\mathbf{M}_{w,x}^{d}(\mathbf{\Sigma}_{w,x} + \boldsymbol{\mu}_{w,x}\boldsymbol{\mu}_{w,x}^{\mathcal{T}})\right) \ \text{ s.t. } A_{w,x} \geq \max\{0, \hat{f}_{w,x}(\mathbf{t}_{r_{w,x}}) - \nu_{w,x}\}, \tag{56}$$

where we define the dual variables $m_{w,x}^{0} \in \mathbb{R}$, $\mathbf{m}_{w,m} \in \mathbb{R}^{(2N_t+2N+1)}$, $\mathbf{m}_{w,U} \in \mathbb{R}^{(2N_r+2N_rN_t+1)}$, $\mathbf{M}_{w,m}^{d} \in \mathbb{R}_{\mathbb{S}}^{(2N_t+2N+1)}$, and $\mathbf{M}_{w,U}^{d} \in \mathbb{R}_{\mathbb{S}}^{(2N_r+2N_rN_t+1)}$ to those equality constraints in problem (55). Therefore, the above problem can be reduced to

$$\begin{aligned} \inf_{\mathbf{M}_{w,x}} \quad & \text{Tr}\left(\mathbf{\Omega}_{w,x}\mathbf{M}_{w,x}\right) \\ \text{s.t.} \quad & \left[\mathbf{t}_{r_{w,x}}^{\mathcal{T}}, 1\right]\mathbf{M}_{w,x}\left[\mathbf{t}_{r_{w,x}}^{\mathcal{T}}, 1\right]^{\mathcal{T}} \geq \max\left\{0, \hat{f}_{w,x}(\mathbf{t}_{r_{w,x}}) - \nu_{w,x}\right\}, \quad \mathbf{M}_{w,x} = \begin{bmatrix} \mathbf{M}_{w,x}^{d} & \frac{1}{2}\mathbf{m}_{w,x} \\ \frac{1}{2}\mathbf{m}_{w,x}^{\mathcal{T}} & m_{w,x}^{0} \end{bmatrix}. \end{aligned} \tag{57}$$

We notice that the semi-infinite constraints for maximization operation can be decoupled into two equivalent constraints, i.e., either greater than zero or $\hat{f}_{w,x}(\mathbf{t}_{r_{w,x}}) - \nu_{w,x}$. As a result, problem (57) becomes

$$\inf_{\mathbf{M}_{w,x}} \quad \text{Tr}\left(\mathbf{\Omega}_{w,x}\mathbf{M}_{w,x}\right) \quad \text{s.t.} \ \left[\mathbf{t}_{r_{w,x}}^{\mathcal{T}}, 1\right]\mathbf{M}_{w,x}\left[\mathbf{t}_{r_{w,x}}^{\mathcal{T}}, 1\right]^{\mathcal{T}} \geq \hat{f}_{w,x}(\mathbf{t}_{r_{w,x}}) - \nu_{w,x}, \quad \mathbf{M}_{w,x} \succeq 0. \tag{58}$$

Since $\hat{f}_{w,x}(\mathbf{t}_{r_{w,x}}) = -f_{w,x}(\mathbf{t}_{r_{w,x}})$ is in a quadraic form, the constraint (58) can be expressed in an LMI form given by

$$\left[\mathbf{t}_{r_{w,x}}^{\mathcal{T}}, 1\right] \left(\mathbf{M}_{w,x} - \begin{bmatrix} \hat{\mathbf{Q}}_{w,x}(\mathbf{W}) & \frac{\hat{\mathbf{q}}_{w,x}(\mathbf{W})^{\mathcal{T}}}{2} \\ \frac{\hat{\mathbf{q}}_{w,x}(\mathbf{W})}{2} & \hat{q}^0_{w,x}(\mathbf{W}) - \nu_{w,x} \end{bmatrix} \right) \left[\mathbf{t}_{r_{w,x}}^{\mathcal{T}}, 1\right]^{\mathcal{T}} \geq 0 \Leftrightarrow \mathbf{M}_{w,x} - \begin{bmatrix} \hat{\mathbf{Q}}_{w,x}(\mathbf{W}) & \frac{\hat{\mathbf{q}}_{w,x}(\mathbf{W})^{\mathcal{T}}}{2} \\ \frac{\hat{\mathbf{q}}_{w,x}(\mathbf{W})}{2} & \hat{q}^0_{w,x}(\mathbf{W}) - \nu_{w,x} \end{bmatrix} \succeq 0. \tag{59}$$

Note that $\hat{\mathbf{Q}}_{w,x}(\mathbf{W}) = -\mathbf{Q}_{w,x}(\mathbf{W})$, $\hat{\mathbf{q}}_{w,x}(\mathbf{W}) = -\mathbf{q}_{w,x}(\mathbf{W})$, and $\hat{q}^0_{w,x}(\mathbf{W}) = -q^0_{w,x}(\mathbf{W})$. Using (59) allows us to reformulate (58) as

$$\inf_{\mathbf{M}_{w,x}} \quad \mathrm{Tr}\left(\mathbf{\Omega}_{w,x}\mathbf{M}_{w,x}\right) \tag{60a}$$

$$\text{s.t.} \;\; \mathbf{M}_{w,x} \succeq 0, \quad \mathbf{M}_{w,x} - \begin{bmatrix} \hat{\mathbf{Q}}_{w,x}(\mathbf{W}) & \frac{\hat{\mathbf{q}}_{w,x}(\mathbf{W})^{\mathcal{T}}}{2} \\ \frac{\hat{\mathbf{q}}_{w,x}(\mathbf{W})}{2} & \hat{q}^0_{w,x}(\mathbf{W}) - \nu_{w,x} \end{bmatrix} \succeq 0.. \tag{60b}$$

Accordingly, replacing the worst-case CVaR problem in (54) by (60) yields

$$\sup_{\mathfrak{D}\in\mathcal{P}} \mathfrak{D}\text{-CVaR}_{\epsilon_x}\left(\hat{f}_{w,x}(\mathbf{t}_{r_{w,x}})\right) = \inf_{\mathbf{M}_{w,x},\nu_{w,x}} \nu_{w,x} + \frac{1}{\epsilon_x}\langle \mathbf{\Omega}_{w,x}, \mathbf{M}_{w,x}\rangle \quad \text{s.t.} \;\; (60b). \tag{61}$$

Moreover, substituting (51) by problem (61) yields

$$\sup_{\mathfrak{D}\in\mathcal{P}} \mathfrak{D}\text{-CVaR}_{\epsilon_x}\left(\hat{f}_{w,x}(\mathbf{t}_{r_{w,x}})\right) \leq 0 \;\Leftrightarrow\; 0 \geq \inf_{\mathbf{M}_{w,x},\nu_{w,x}} \nu_{w,x} + \frac{1}{\epsilon_x}\langle \mathbf{\Omega}_{w,x}, \mathbf{M}_{w,x}\rangle \quad \text{s.t.} \;\; (60b), \tag{62}$$

which is complied with (52). This completes the proof. □

Therefore, based on proposition (1), the problem of robust optimization in (35) becomes

$$\max_{\mathbf{W},\overline{\gamma}_D,\mathbf{M}_{w,x},\nu_{w,x},\forall x\in\{m,U\}} \quad \sum_{m\in\mathcal{M}} \overline{\gamma}_{D,m} \tag{63a}$$

$$\text{s.t. } \mathbf{M}_{w,x} \succeq 0, \quad \forall x \in \{m, U\}, \tag{63b}$$

$$\nu_{w,x} + \frac{1}{\epsilon_x}\mathrm{Tr}\left(\mathbf{\Omega}_{w,x}\mathbf{M}_{w,x}\right) \leq 0, \quad \forall x \in \{m, U\}, \tag{63c}$$

$$\mathbf{M}_{w,x} - \begin{bmatrix} \hat{\mathbf{Q}}_{w,x}\left(\mathbf{W}\right) & \frac{\hat{\mathbf{q}}_{w,x}(\mathbf{W})^{\mathcal{T}}}{2} \\ \frac{\hat{\mathbf{q}}_{w,x}(\mathbf{W})}{2} & \hat{q}^0_{w,x}\left(\mathbf{W}\right) - \nu_{w,x} \end{bmatrix} \succeq 0, \quad \forall x \in \{m, U\}, \tag{63d}$$

$$\sum_{m\in\mathcal{M}} \mathbf{w}_m^{\mathcal{H}}\mathbf{w}_m \leq P_{\max}. \tag{63e}$$

From the matrix in (63d), the active beamforming parameter can be alternatively expressed by a matrix form as $\mathbf{W}_{t,m} = \mathbf{w}_m\mathbf{w}_m^{\mathcal{H}} \in \mathbb{C}^{N_t\times N_t}$. Accordingly, we rewrite the inequalities for DL and UL constraint in (63d) with all parameters in (39) and (44) w.r.t. $\mathbf{W}_{t,m}$. Note that in $q^0_{w,m}(\mathbf{W})$ we have $\mathbf{w}_m^{\mathcal{H}}\mathbf{D}_m^{\mathcal{H}}\mathbf{D}_m\mathbf{w}_m = \mathbf{D}_m\mathbf{w}_m\mathbf{w}_m^{\mathcal{H}}\mathbf{D}_m^{\mathcal{H}} = \mathbf{D}_m\mathbf{W}_{w,m}\mathbf{D}_m^{\mathcal{H}}$. We neglect the remaining parameter transformation to prevent repeated definitions. We can infer that there exists another form of beamforming matrix, i.e., $\mathbf{w}_n\mathbf{w}_{m'}^{\mathcal{H}}, \forall n \neq m'$ in $\mathbf{\Xi}_{w,S}$ and $\mathbf{\Upsilon}_{w,S}$, which leads to an unsolvable solution. Therefore, we readily apply additional AO with

the solution at previous iteration of $\mathbf{w}_n^{(p)}\mathbf{w}_{m'}^{(p)\mathcal{H}}$ rather than $\mathbf{w}_n\mathbf{w}_{m'}^{\mathcal{H}}$, where p indicates the previous iteration index of active beamforming. Moreover, we can equivalently convert $\mathbf{w}_m^{\mathcal{H}}\mathbf{w}_m$ in (63e) into the constraints in a matrix form given by

$$\mathbf{W}_{t,m} \succeq 0,\ \text{rank}(\mathbf{W}_{t,m}) = 1,\ \mathbf{W}_{t,m} = \mathbf{W}_{t,m}^{\mathcal{H}}, \tag{64}$$

where $\text{rank}(\cdot)$ indicates the rank of a matrix. However, the objective regarding DL SINR threshold $\overline{\gamma}_{D,m}, \forall m \in \mathcal{M}$ is coupled with the beamforming matrix $\mathbf{W}_{t,m}, \forall m \in \mathcal{M}$. Hence, we iteratively solve the optimization for the DL UE m with other fixed parameters for DL UE $m' \neq m$. Accordingly, the final subproblem for optimizing active BS beamforming for DL UE m is formulated as

$$\max_{\mathbf{W}_{t,m},\overline{\gamma}_{D,m},\mathbf{M}_{w,m},\mathbf{M}_{w,U},\nu_{w,m},\nu_{w,U}} \quad \overline{\gamma}_{D,m} \tag{65a}$$

$$\text{s.t. } \mathbf{M}_{w,m} \succeq 0, \quad \nu_{w,m} + \frac{1}{\epsilon_m}\text{Tr}\left(\mathbf{\Omega}_{w,m}\mathbf{M}_{w,m}\right) \leq 0, \quad \mathbf{M}_{w,m} - \begin{bmatrix} \hat{\mathbf{Q}}_{w,m}(\mathbf{W}_{t,m}) & \frac{\hat{\mathbf{q}}_{w,m}(\mathbf{W}_{t,m})^{\mathcal{T}}}{2} \\ \frac{\hat{\mathbf{q}}_{w,m}(\mathbf{W}_{t,m})}{2} & \hat{q}_{w,m}^0(\mathbf{W}_{t,m}) - \nu_{w,m} \end{bmatrix} \succeq 0, \tag{65b}$$

$$\mathbf{M}_{w,U} \succeq 0, \quad \nu_{w,U} + \frac{1}{\epsilon_U}\text{Tr}\left(\mathbf{\Omega}_{w,U}\mathbf{M}_{w,U}\right) \leq 0, \quad \mathbf{M}_{w,U} - \begin{bmatrix} \hat{\mathbf{Q}}_{w,U}(\mathbf{W}_{t,m}) & \frac{\hat{\mathbf{q}}_{w,U}(\mathbf{W}_{t,m})^{\mathcal{T}}}{2} \\ \frac{\hat{\mathbf{q}}_{w,U}(\mathbf{W}_{t,m})}{2} & \hat{q}_{w,U}^0(\mathbf{W}_{t,m}) - \nu_{w,U} \end{bmatrix} \succeq 0, \tag{65c}$$

$$\text{Tr}\left(\mathbf{W}_{t,m}\right) \leq \frac{P_{\text{max}}}{M}, \tag{65d}$$

$$\mathbf{W}_{t,m} \succeq 0,\ \text{rank}(\mathbf{W}_{t,m}) = 1,\ \mathbf{W}_{t,m} = \mathbf{W}_{t,m}^{\mathcal{H}}. \tag{65e}$$

Moreover, we employ semi-definite relaxation (SDR) to drop the non-convex rank-one constraint in (65e). The DL and UL constraints in (65b) and (65c) are in a form of LMI. Moreover, the problem (65) performs SDP, which can be solved via convex optimization tool to obtain the optimum of active BS beamforming with imperfect CSI. To elaborate a little further, SDP may provide non-rank-one solution of $\mathbf{W}_{t,m}$. Ones $\mathbf{W}_{t,m}$ is available and feasible, we employ the Gaussian randomization method [43] to obtain the rank-one $\mathbf{W}_{t,m}$ solution for $\mathbf{w}_m$ to the problem (65). However, when $\mathbf{W}_{t,m}$ performs a non-rank-one solution, we should adopt the eigenvalue decomposition, i.e., $\mathbf{X} = \mathbf{Y}\mathbf{\Lambda}\mathbf{Y}^{\mathcal{H}}$ where $\mathbf{Y}$ and $\mathbf{\Lambda}$ stand for unitary and diagonal matrix, respectively. As a result, the suboptimal solution is obtained in a form of $\mathbf{Y}\mathbf{\Lambda}^{\frac{1}{2}}\mathbf{g}$, where $\mathbf{g} \sim \mathcal{CN}(\mathbf{0}, \mathbf{I})$ denotes a randomized complex Gaussian eigenvector.

C. Optimization of Passive RIS Beamforming with Imperfect CSI

After obtaining the optimal active beamforming of $\mathbf{W}^*$, the original problem (34) becomes

$$\max_{\boldsymbol{\Theta},\boldsymbol{\gamma}_D} \sum_{m\in\mathcal{M}} \gamma_{D,m} \tag{66a}$$

$$\text{s.t.} \inf_{\mathfrak{D}\in\mathcal{P}} \mathbb{P}_{\mathfrak{D}}\{\log_2(1+\text{SINR}_{D,m}^{r,\theta}) \geq \gamma_{D,m}\} \geq 1-\epsilon_m, \forall m, \tag{66b}$$

$$\inf_{\mathfrak{D}\in\mathcal{P}} \mathbb{P}_{\mathfrak{D}}\{\log_2(1+\text{SINR}_{U}^{r,\theta}) \geq \gamma_{U}\} \geq 1-\epsilon_U, \tag{66c}$$

$$(11c), (34d), \tag{66d}$$

where $\text{SINR}_{D,m}^{r,\theta} = \frac{\|(\mathbf{D}_m+(\widetilde{\mathbf{D}}_{t_m}+\triangle\mathbf{D}_{t_m})\boldsymbol{\Theta}^{(D)})\mathbf{w}_m^*\overline{x}_{D,m}\|^2}{\sum_{m'\in\mathcal{M}\setminus m}\|(\mathbf{D}_m+(\widetilde{\mathbf{D}}_{t_m}+\triangle\mathbf{D}_{t_m})\boldsymbol{\Theta}^{(D)})\mathbf{w}_{m'}^*\overline{x}_{D,m'}\|^2+\|(\mathbf{V}_m+(\widetilde{\mathbf{C}}_{t_m}+\triangle\mathbf{C}_{t_m})\boldsymbol{\Theta}^{(D)})\overline{\mathbf{x}}_U\|^2+\sigma^2}$ and $\text{SINR}_{U}^{r,\theta} = \frac{\|(\mathbf{U}+(\widetilde{\mathbf{U}}_t+\triangle\mathbf{U}_t)\boldsymbol{\Theta}^{(U)})\overline{\mathbf{x}}_U\|^2}{\|(\mathbf{S}+(\widetilde{\mathbf{S}}_t+\triangle\mathbf{S}_t)\boldsymbol{\Theta}^{(U)})\mathbf{W}^*\overline{\mathbf{x}}_D\|^2+\sigma^2}$. Note that in the following derivation we use vector form of RIS $\boldsymbol{\theta}$ in replace of matrix one $\boldsymbol{\Theta}$. Similar to the reformulation in (36), we have

$$\text{SINR}_{D,m}^{r,\theta} \geq \overline{\gamma}_{D,m} \Rightarrow \frac{p_D\|\mathbf{D}_m\mathbf{w}_m^*+\ddot{\mathbf{D}}_{t_m}\boldsymbol{\theta}\|^2}{\sum_{m'\in\mathcal{M}\setminus m}p_D\|\mathbf{D}_m\mathbf{w}_{m'}^*+\ddot{\mathbf{D}}_{t_m}\boldsymbol{\theta}\|^2+\|\mathbf{V}_m\overline{\mathbf{x}}_U+\ddot{\mathbf{C}}_{t_m}\boldsymbol{\theta}\|^2+n_m} \geq \overline{\gamma}_{D,m}, \tag{67}$$

where $\ddot{\mathbf{D}}_{t_m} = (\widetilde{\mathbf{D}}_{t_m}+\triangle\mathbf{D}_{t_m})\mathbf{w}_m^{*(D)}$ and $\ddot{\mathbf{C}}_{t_m} = (\widetilde{\mathbf{C}}_{t_m}+\triangle\mathbf{C}_{t_m})\overline{\mathbf{x}}_U$. We denote $\mathbf{t}_{r_{\theta,m}} \in \mathbb{R}^{1\times 6K}$ as random channel error as

$$\mathbf{t}_{r_{\theta,m}} = \left[\text{Re}\{\ddot{\mathbf{D}}_{t_m}\}, \text{Im}\{\ddot{\mathbf{D}}_{t_m}\}, \text{Re}\{\ddot{\mathbf{D}}_{t_{-m}}\}, \text{Im}\{\ddot{\mathbf{D}}_{t_{-m}}\}, \text{Re}\{\ddot{\mathbf{C}}_{t_m}\}, \text{Im}\{\ddot{\mathbf{C}}_{t_m}\}\right], \tag{68}$$

where $\ddot{\mathbf{D}}_{t_{-m}} = \sum_{m'\in\mathcal{M}\setminus m}\mathbf{D}_{t_m}\mathbf{w}_{m'}^*$. Assume that $f_{\theta,m}(\mathbf{t}_{r_{\theta,m}}) : \mathbb{R}^{1\times 6K} \to \mathbb{R}$ and (67) becomes

$$f_{\theta,m}(\mathbf{t}_{r_{\theta,m}}) \geq 0, \Rightarrow \mathbf{t}_{r_{\theta,m}}\mathbf{Q}_{\theta,m}(\boldsymbol{\theta})\mathbf{t}_{r_{\theta,m}}^{\mathcal{T}} + 2\mathbf{q}_{\theta,m}(\boldsymbol{\theta})\mathbf{t}_{r_{\theta,m}}^{\mathcal{T}} + q_{\theta,m}^0 \geq 0, \tag{69}$$

where

$$\mathbf{Q}_{\theta,m}(\boldsymbol{\theta}) = \begin{bmatrix} \text{Re}\{\boldsymbol{\Upsilon}_{\theta,m}\} & \text{Im}\{\boldsymbol{\Upsilon}_{\theta,m}\} & \mathbf{0} & \mathbf{0} & \mathbf{0} & \mathbf{0} \\ -\text{Im}\{\boldsymbol{\Upsilon}_{\theta,m}\} & \text{Re}\{\boldsymbol{\Upsilon}_{\theta,m}\} & \mathbf{0} & \mathbf{0} & \mathbf{0} & \mathbf{0} \\ \mathbf{0} & \mathbf{0} & \text{Re}\{\boldsymbol{\Upsilon}_{\theta,-m}\} & \text{Im}\{\boldsymbol{\Upsilon}_{\theta,-m}\} & \mathbf{0} & \mathbf{0} \\ \mathbf{0} & \mathbf{0} & -\text{Im}\{\boldsymbol{\Upsilon}_{\theta,-m}\} & \text{Re}\{\boldsymbol{\Upsilon}_{\theta,-m}\} & \mathbf{0} & \mathbf{0} \\ \mathbf{0} & \mathbf{0} & \mathbf{0} & \mathbf{0} & \text{Re}\{\boldsymbol{\Upsilon}_{\theta,V_m}\} & \text{Im}\{\boldsymbol{\Upsilon}_{\theta,V_m}\} \\ \mathbf{0} & \mathbf{0} & \mathbf{0} & \mathbf{0} & -\text{Im}\{\boldsymbol{\Upsilon}_{\theta,V_m}\} & \text{Re}\{\boldsymbol{\Upsilon}_{\theta,V_m}\} \end{bmatrix} \in \mathbb{R}^{6K\times 6K},$$

$$\mathbf{q}_{\theta,m}(\boldsymbol{\theta}) = [\text{Re}\{\boldsymbol{\Xi}_{\theta,m}\}, \text{Im}\{\boldsymbol{\Xi}_{\theta,m}\}, \text{Re}\{\boldsymbol{\Xi}_{\theta,-m}\}, \text{Im}\{\boldsymbol{\Xi}_{\theta,-m}\}, \text{Re}\{\boldsymbol{\Xi}_{\theta,V_m}\}, \text{Im}\{\boldsymbol{\Xi}_{\theta,V_m}\}] \in \mathbb{R}^{1\times 6K},$$

$$q_{\theta,m}^0 = p_D(\mathbf{w}_m^*)^{\mathcal{H}}\mathbf{D}_m^{\mathcal{H}}\mathbf{D}_m\mathbf{w}_m^* - \overline{\gamma}_{D,m}\left(\sum_{m'\in\mathcal{M}\setminus m} p_D(\mathbf{w}_{m'}^*)^{\mathcal{H}}\mathbf{D}_m^{\mathcal{H}}\mathbf{D}_m\mathbf{w}_{m'}^* + \overline{\mathbf{x}}_U^{\mathcal{H}}\mathbf{V}_m^{\mathcal{H}}\mathbf{V}_m\overline{\mathbf{x}}_U + \sigma^2\right) \in \mathbb{R}, \tag{70}$$

where $\boldsymbol{\Upsilon}_{\theta,m} = \boldsymbol{\theta}\boldsymbol{\theta}^{\mathcal{H}}$, $\boldsymbol{\Upsilon}_{\theta,-m} = -\overline{\gamma}_{D,m}\boldsymbol{\theta}\boldsymbol{\theta}^{\mathcal{H}}$, $\boldsymbol{\Upsilon}_{\theta,V_m} = \boldsymbol{\theta}\boldsymbol{\theta}^{\mathcal{H}}$, $\boldsymbol{\Xi}_{\theta,m} = \mathbf{D}_m\mathbf{w}_m^*\boldsymbol{\theta}^{\mathcal{H}}$, $\boldsymbol{\Xi}_{\theta,-m} = -\overline{\gamma}_{D,m}\sum_{m'\in\mathcal{M}\setminus m}\mathbf{D}_m\mathbf{w}_{m'}^*\boldsymbol{\theta}^{\mathcal{H}}$, and $\boldsymbol{\Xi}_{\theta,V_m} = \mathbf{V}_m\overline{\mathbf{x}}_U\boldsymbol{\theta}^{\mathcal{H}}$. Therefore, the DL constraint (66b) can be rewritten as

$$\inf_{\mathfrak{D}\in\mathcal{P}} \mathbb{P}_{\mathfrak{D}}\{f_{\theta,m}(\mathbf{t}_{r_{\theta,m}}) \geq 0\} \geq 1-\epsilon_m. \tag{71}$$

As for UL, we can reformulate the inequality as

$$\text{SINR}_U^{r,\theta} \geq \overline{\gamma}_U \Rightarrow \frac{\|\mathbf{U}\overline{\mathbf{x}}_U + \boldsymbol{\Theta}^{(U)'}\ddot{\mathbf{U}}_t\|^2}{\|\mathbf{S}\mathbf{W}^*\overline{\mathbf{x}}_D + \boldsymbol{\Theta}^{(U)'}\ddot{\mathbf{S}}_t\|^2+\sigma^2} \geq \overline{\gamma}_U, \tag{72}$$

where $\ddot{\mathbf{U}}_t = [\dot{u}_{1,1}, ..., \dot{u}_{N_r,1}, \dot{u}_{1,2}, ..., \dot{u}_{N_r,2}, ..., \dot{u}_{1,K}, ..., \dot{u}_{N_r,K}]^{\mathcal{T}} \in \mathbb{C}^{KN_r}$, $\dot{u}_{n_r,k} = \mathbf{U}_{t_{n_r,k}}\overline{\mathbf{x}}_U \in \mathbb{C}$, $\ddot{\mathbf{S}}_t = [\dot{s}_{1,1}, ..., \dot{s}_{N_r,1}, \dot{s}_{1,2}, ..., \dot{s}_{N_r,2}, ..., \dot{s}_{1,K}, ..., \dot{s}_{N_r,K}] \in \mathbb{C}^{KN_r}$, $\dot{s}_{n_r,k} = \mathbf{S}_{t_{n_r,k}}\mathbf{W}^*\overline{\mathbf{x}}_D \in \mathbb{C}$, and $\boldsymbol{\Theta}^{(U)'} = [\mathbf{E}_{U',1}, \mathbf{E}_{U',2}, ..., \mathbf{E}_{U',K}] \in \mathbb{R}^{N_r \times KN_r}$. Note that $\mathbf{U}_{t_{n_r,k}} \in \mathbb{R}^{1\times N}$ is row vector of row n_r and column from $(k-1)N+1$ to kN in $\mathbf{U}_t$, whilst $\mathbf{S}_{t_{n_r,k}} \in \mathbb{R}^{1\times N_t}$ is a row vector of row n_r and column from $(k-1)N_t+1$ to kN_t in $\mathbf{S}_t$. We define $\mathbf{E}_{U',k} = e^{-j\theta_k}\mathbf{I}_{N_r} \in \mathbb{R}^{N_r\times N_r}$. Then, we define $\mathbf{t}_{r_{\theta,U}} \in \mathbb{R}^{1\times 4KN_r}$ as the random channel error for the UL constraint as

$$\mathbf{t}_{r_{\theta,U}} = [\text{Re}\{\ddot{\mathbf{U}}_t\}, \text{Im}\{\ddot{\mathbf{U}}_t\}, \text{Re}\{\ddot{\mathbf{S}}_t\}, \text{Im}\{\ddot{\mathbf{S}}_t\}]. \tag{73}$$

Assume that $f_{\theta,U}(\mathbf{t}_{r_{\theta,U}}) : \mathbb{R}^{1\times 4KN_r} \to \mathbb{R}$, we are able to reformulate (72) as

$$f_{\theta,U}(\mathbf{t}_{r_{\theta,U}}) \geq 0 \Rightarrow \mathbf{t}_{r_{\theta,U}}\mathbf{Q}_{\theta,U}(\boldsymbol{\theta})\mathbf{t}_{r_{\theta,U}}^{\mathcal{T}} + 2\mathbf{q}_{\theta,U}(\boldsymbol{\theta})\mathbf{t}_{r_{\theta,U}}^{\mathcal{T}} + q_{\theta,U}^0 \geq 0, \tag{74}$$

where

$$\begin{aligned}
\mathbf{Q}_{\theta,U}(\boldsymbol{\theta}) &= \begin{bmatrix} \text{Re}\{\boldsymbol{\Upsilon}_{\theta,C}\} & \text{Im}\{\boldsymbol{\Upsilon}_{\theta,C}\} & \mathbf{0} & \mathbf{0} \\ -\text{Im}\{\boldsymbol{\Upsilon}_{\theta,C}\} & \text{Re}\{\boldsymbol{\Upsilon}_{\theta,C}\} & \mathbf{0} & \mathbf{0} \\ \mathbf{0} & \mathbf{0} & \text{Re}\{\boldsymbol{\Upsilon}_{\theta,S}\} & \text{Im}\{\boldsymbol{\Upsilon}_{\theta,S}\} \\ \mathbf{0} & \mathbf{0} & -\text{Im}\{\boldsymbol{\Upsilon}_{\theta,S}\} & \text{Re}\{\boldsymbol{\Upsilon}_{\theta,S}\} \end{bmatrix} \in \mathbb{R}^{4KN_r\times 4KN_r}, \\
\mathbf{q}_{\theta,U}(\boldsymbol{\theta}) &= [\text{Re}\left\{\boldsymbol{\Xi}_{\theta,C}\right\}, \text{Im}\left\{\boldsymbol{\Xi}_{\theta,C}\right\}, \text{Re}\left\{\boldsymbol{\Xi}_{\theta,S}\right\}, \text{Im}\left\{\boldsymbol{\Xi}_{\theta,S}\right\}] \in \mathbb{R}^{1\times 4KN_r}, \\
q_{\theta,U}^0 &= \overline{\mathbf{x}}_U^{\mathcal{H}}\mathbf{U}^{\mathcal{H}}\mathbf{U}\overline{\mathbf{x}}_U - \overline{\gamma}_U\left(\overline{\mathbf{x}}_D^{\mathcal{H}}(\mathbf{W}^*)^{\mathcal{H}}\mathbf{S}^{\mathcal{H}}\mathbf{S}\mathbf{W}^*\overline{\mathbf{x}}_D + \sigma^2\right) \in \mathbb{R},
\end{aligned} \tag{75}$$

where related parameters in $\mathbf{Q}_{\theta,U}(\boldsymbol{\theta})$ and $\mathbf{q}_{\theta,U}(\boldsymbol{\theta})$ are defined as follows.

$$\begin{aligned}
\boldsymbol{\Upsilon}_{\theta,C} &= (\boldsymbol{\Theta}^{(U)'})^{\mathcal{H}}\boldsymbol{\Theta}^{(U)'} = \begin{bmatrix} \mathbf{I}_{N_r} & e^{j(\theta_1-\theta_2)}\mathbf{I}_{N_r} & \cdots & e^{j(\theta_1-\theta_K)}\mathbf{I}_{N_r} \\ e^{j(\theta_2-\theta_1)}\mathbf{I}_{N_r} & \mathbf{I}_{N_r} & \cdots & e^{j(\theta_2-\theta_K)}\mathbf{I}_{N_r} \\ \vdots & \vdots & \ddots & \vdots \\ e^{j(\theta_K-\theta_1)}\mathbf{I}_{N_r} & e^{j(\theta_K-\theta_2)}\mathbf{I}_{N_r} & \cdots & \mathbf{I}_{N_r} \end{bmatrix} = \boldsymbol{\theta}\boldsymbol{\theta}^{\mathcal{H}} \otimes \mathbf{I}_{N_r}, \\
\boldsymbol{\Upsilon}_{\theta,S} &= -\overline{\gamma}_U\boldsymbol{\Upsilon}_{\theta,C}, \quad \boldsymbol{\Xi}_{\theta,C} = \overline{\mathbf{x}}_U^{\mathcal{H}}\mathbf{U}^{\mathcal{H}}\boldsymbol{\Theta}^{(U)'}, \quad \boldsymbol{\Xi}_{\theta,S}^r = -\overline{\gamma}_U\overline{\mathbf{x}}_D^{\mathcal{H}}\mathbf{W}^{*^{\mathcal{H}}}\mathbf{S}^{\mathcal{H}}\boldsymbol{\Theta}^{(U)'}.
\end{aligned} \tag{76}$$

Accordingly, we can obtain the UL chance constraint (66c) as

$$\inf_{\mathfrak{D}\in\mathcal{P}} \mathbb{P}_{\mathfrak{D}}\{f_{\theta,U}(\mathbf{t}_{r_{\theta,U}}) \geq 0\} \geq 1 - \epsilon_U. \tag{77}$$

Based on Lemma 1 and Proposition 2, the constraints of (71) and (77) can be equivalently transformed into the following constraint set as

$$\left\{ \begin{aligned} &\mathbf{M}_{\theta,x} \succeq 0, \nu_{\theta,x} + \frac{1}{\epsilon_x}\text{Tr}\left(\boldsymbol{\Omega}_{\theta,x}\mathbf{M}_{\theta,x}\right) \leq 0, \\ &\mathbf{M}_{\theta,x} - \begin{bmatrix} \hat{\mathbf{Q}}_{\theta,x}(\boldsymbol{\theta}) & \frac{\hat{\mathbf{q}}_{\theta,x}(\boldsymbol{\theta})^{\mathcal{T}}}{2} \\ \frac{\hat{\mathbf{q}}_{\theta,x}(\boldsymbol{\theta})}{2} & \hat{q}_{\theta,x}^0 - \nu_{\theta,x} \end{bmatrix} \succeq 0. \end{aligned} \right\}, \tag{78}$$

where $\nu_{\theta,x}$ represents the risk threshold w.r.t. passive RIS beamforming, $\mathbf{\Omega}_{\theta,x}$ indicates the second-order moment matrix of $\mathbf{t}_{r_{\theta,x}}$, and $\mathbf{M}_{\theta,x}$ denotes the dual variable matrix, which are defined with the identical structure in (47), (53), and (57), respectively. Also, $\hat{\mathbf{Q}}_{\theta,x}(\boldsymbol{\theta}) = -\mathbf{Q}_{\theta,x}(\boldsymbol{\theta})$, $\hat{\mathbf{q}}_{\theta,x}(\boldsymbol{\theta}) = -\mathbf{q}_{\theta,x}(\boldsymbol{\theta})$, and $\hat{q}^0_{\theta,x} = -q^0_{\theta,x}$ Therefore, the robust beamforming problem (66) now becomes

$$\max_{\boldsymbol{\theta},\overline{\boldsymbol{\gamma}}_D,\mathbf{M}_{\theta,x},\nu_{\theta,x},\forall x\in\{m,U\}} \sum_{m\in\mathcal{M}} \overline{\gamma}_{D,m} \tag{79a}$$

$$\text{s.t. (11c), (78).} \tag{79b}$$

Then, we define the RIS phase-shift variable in a matrix expression as $\mathbf{P} = \boldsymbol{\theta}\boldsymbol{\theta}^{\mathcal{H}}$. Note that we neglect the repeated notational definitions w.r.t. $\mathbf{P}$. We can infer that the problem (79) is unsolvable since it contains the RIS parameter in both forms of vector in $\hat{\mathbf{q}}_{\theta,m}(\mathbf{P})$ and matrix in $\hat{\mathbf{Q}}_{\theta,m}(\mathbf{P})$. Therefore, we convert the third constraint in (78) as

$$\begin{aligned} &\mathbf{M}_{\theta,x} - \begin{bmatrix} \hat{\mathbf{Q}}_{\theta,x}(\mathbf{P}) & \mathbf{0} \\ \mathbf{0} & \hat{q}^0_{\theta,x}-\nu_{\theta,x} \end{bmatrix} \succeq \begin{bmatrix} \mathbf{0} & \frac{\hat{\mathbf{q}}_{\theta,x}(\mathbf{P})^{\mathcal{T}}}{2} \\ \mathbf{0} & 0 \end{bmatrix} + \begin{bmatrix} \mathbf{0} & \mathbf{0} \\ \frac{\hat{\mathbf{q}}_{\theta,x}(\mathbf{P})}{2} & 0 \end{bmatrix} \\ &\Rightarrow \mathbf{M}^t_{\theta,x} \succeq \left(\mathbf{H}^{\mathcal{H}}_{1,\theta,x}\mathbf{\Lambda}_{1,\theta,x} + \mathbf{\Lambda}^{\mathcal{H}}_{1,\theta,x}\mathbf{H}_{1,\theta,x}\right) + \left(\mathbf{H}^{\mathcal{H}}_{2,\theta,x}\mathbf{\Lambda}_{2,\theta,x} + \mathbf{\Lambda}^{\mathcal{H}}_{2,\theta,x}\mathbf{H}_{2,\theta,x}\right), \end{aligned} \tag{80}$$

where we define pertinent parameters as follows.

$$\mathbf{M}^t_{\theta,x} = \mathbf{M}_{\theta,x} - \begin{bmatrix} \hat{\mathbf{Q}}_{\theta,x}(\mathbf{P}) & \mathbf{0} \\ \mathbf{0} & \hat{q}^0_{\theta,x}-\nu_{\theta,x} \end{bmatrix},$$

$$\mathbf{H}_{1,\theta,m} = \begin{bmatrix} \mathbf{0} & \mathbf{0} & \mathbf{0} & \mathbf{0} & \mathbf{0} & \mathbf{0} \\ \frac{\mathbf{D}_m(\mathbf{w}^*_m)^\dagger}{-2} & \frac{\mathbf{D}_m(\mathbf{w}^*_m)^\dagger}{-2j} & \frac{\mathbf{D}_m(\mathbf{w}^*_{-m})^\dagger}{-2} & \frac{\mathbf{D}_m(\mathbf{w}^*_{-m})^\dagger}{-2j} & \frac{\mathbf{V}_m\overline{\mathbf{x}}_U}{-2} & \frac{\mathbf{V}_m\overline{\mathbf{x}}_U}{-2j} \end{bmatrix}^{\mathcal{H}} \in \mathbb{C}^{6\times(6K+1)},$$

$$\mathbf{H}_{2,\theta,m} = \begin{bmatrix} \mathbf{0} & \mathbf{0} & \mathbf{0} & \mathbf{0} & \mathbf{0} & \mathbf{0} \\ \frac{\mathbf{D}^\dagger_m\mathbf{w}^*_m}{-2} & \frac{\mathbf{D}^\dagger_m\mathbf{w}^*_m}{2j} & \frac{\mathbf{D}^\dagger_m\mathbf{w}^*_{-m}}{-2} & \frac{\mathbf{D}^\dagger_m\mathbf{w}^*_{-m}}{2j} & \frac{\mathbf{V}^\dagger_m\overline{\mathbf{x}}_U}{-2} & \frac{\mathbf{V}^\dagger_m\overline{\mathbf{x}}_U}{2j} \end{bmatrix}^{\mathcal{H}} \in \mathbb{C}^{6\times(6K+1)},$$

$$\mathbf{H}_{1,\theta,U} = \begin{bmatrix} \mathbf{0} & \mathbf{0} & \mathbf{0} & \mathbf{0} \\ \frac{\overline{\mathbf{x}}_{U,t}}{-2} & \frac{\overline{\mathbf{x}}_{U,t}}{-2j} & \frac{\overline{\mathbf{x}}_{D,t}}{-2} & \frac{\overline{\mathbf{x}}_{D,t}}{-2j} \end{bmatrix}^{\mathcal{H}} \in \mathbb{C}^{4K\times(4N_rK+1)}, \quad \mathbf{H}_{2,\theta,U} = \begin{bmatrix} \mathbf{0} & \mathbf{0} & \mathbf{0} & \mathbf{0} \\ \frac{\overline{\mathbf{x}}^\dagger_{U,t}}{-2} & \frac{\overline{\mathbf{x}}^\dagger_{U,t}}{2j} & \frac{\overline{\mathbf{x}}^\dagger_{D,t}}{-2} & \frac{\overline{\mathbf{x}}^\dagger_{D,t}}{2j} \end{bmatrix}^{\mathcal{H}} \in \mathbb{C}^{4K\times(4N_rK+1)},$$

$$\mathbf{\Lambda}_{1,\theta,m} = \begin{bmatrix} \left(\boldsymbol{\theta}^{\mathcal{H}} \otimes \mathbf{I}_6\right) & \mathbf{0} \end{bmatrix} \in \mathbb{C}^{6\times(6K+1)}, \quad \mathbf{\Lambda}_{2,\theta,m} = \begin{bmatrix} \left(\boldsymbol{\theta}^{\mathcal{T}} \otimes \mathbf{I}_6\right) & \mathbf{0} \end{bmatrix} \in \mathbb{C}^{6\times(6K+1)},$$

$$\mathbf{\Lambda}_{1,\theta,U} = \begin{bmatrix} \left(\boldsymbol{\theta}^{\mathcal{H}} \otimes \mathbf{I}_4\right) & \mathbf{0} \end{bmatrix} \in \mathbb{C}^{4K\times(4N_rK+1)}, \quad \mathbf{\Lambda}_{2,\theta,U} = \begin{bmatrix} \left(\boldsymbol{\theta}^{\mathcal{T}} \otimes \mathbf{I}_4\right) & \mathbf{0} \end{bmatrix} \in \mathbb{C}^{4K\times(4N_rK+1)}.$$

In the following proposition, we have further equivalent transformation in order to change all RIS parameters into a matrix $\mathbf{P}$. Based on sign-definiteness in [44], we have further equivalent transformation in the following proposition.

Proposition 3. *(Sign-Definiteness) The chance constraint* (80) *is equivalent to following constraint*

$$\begin{bmatrix} \mathbf{Z}_{\theta,x}\left(\mathbf{P}, \mathbf{M}_{\theta,x}, \nu_x\right) & -\mathbf{H}^{\mathcal{H}}_{1,\theta,x} & -\mathbf{H}^{\mathcal{H}}_{2,\theta,x} \\ -\mathbf{H}_{1,\theta,x} & \rho_{1,\theta,x}\mathbf{I}_{D_x} & \mathbf{0} \\ -\mathbf{H}_{2,\theta,x} & \mathbf{0} & \rho_{2,\theta,x}\mathbf{I}_{D_x} \end{bmatrix} \succeq 0, \tag{81}$$

where $\rho_{1,\theta,m}, \rho_{2,\theta,m} \geq 0$ *and* $\mathbf{Z}_{\theta,x}\left(\mathbf{P}, \mathbf{M}_{\theta,x}, \nu_x\right) = \mathbf{M}_{\theta,x}^t + \rho_{1,\theta,m}\mathrm{diag}\left((\mathbf{i}_{D_x} \otimes \mathbf{P}), 0\right) + \rho_{2,\theta,m}\mathrm{diag}\left((\mathbf{i}_{D_x} \otimes \mathbf{P}^{\mathcal{H}}), 0\right)$. *Note that* $\mathbf{i}_{D_x}$ *denotes a unit vector with a length of* $D_x, \forall x \in \{m, U\}$ *where* $D_m = 6$ *and* $D_U = 4K$.

Proof. As a simplified version of Lemma 1 in [44] with only two imperfect CSI related variables of $\mathbf{H}_{i,\theta,x}, \forall i \in \{1, 2\}$. In [44], Cauchy-Schwarz inequality and the general form of the $\mathcal{S}$-procedure are adopted for transforming quadratic functions. Due to similar derivation to [44], we neglect the detailed proof here. □

Moreover, to attain an LMI, we employ the Schur complement [45] with symmetric positive-definite matrix to transform (81) into

$$\mathbf{Z}_{\theta,x}(\mathbf{P}, \mathbf{M}_{\theta,x}, \nu_x) - \left[\begin{array}{cc} \mathbf{H}_{1,\theta,x}^{\mathcal{H}} & \mathbf{H}_{2,\theta,x}^{\mathcal{H}} \end{array}\right] \left[\begin{array}{cc} \frac{1}{\rho_{1,\theta,x}}\mathbf{I}_{D_x} & \mathbf{0} \\ \mathbf{0} & \frac{1}{\rho_{2,\theta,x}}\mathbf{I}_{D_x} \end{array}\right] \left[\begin{array}{c} \mathbf{H}_{1,\theta,x} \\ \mathbf{H}_{2,\theta,x} \end{array}\right] \succeq 0, \quad \left[\begin{array}{cc} \rho_{1,\theta,m}\mathbf{I}_{D_x} & \mathbf{0} \\ \mathbf{0} & \rho_{2,\theta,m}\mathbf{I}_{D_x} \end{array}\right] \succeq 0 \tag{82}$$

$$\Rightarrow \mathbf{Z}_{\theta,x}(\mathbf{P}, \mathbf{M}_{\theta,x}, \nu_x) - \left[\begin{array}{cc} \mathbf{0} & \mathbf{0} \\ \mathbf{0} & c_{\rho,x} \end{array}\right] \succeq 0, \quad \rho_{1,\theta,x} \geq 0, \rho_{2,\theta,x} \geq 0, \tag{83}$$

where $c_{\rho,x}$ indicates a constant deriving by computing the norm of the last row of $\mathbf{H}_{1,\theta,x}$ and $\mathbf{H}_{2,\theta,x}$. We neglect the detail of $c_{\rho,x}$ which can be readily derived by expanding equation in (82). Furthermore, for the second inequality of (82) performing a positive semidefinite matrix, the elements on the diagonal is definitely non-negative, resulting in the $\rho_{1,\theta,x}, \rho_{2,\theta,x} \geq 0$ in (83). Therefore, we can obtain an LMI w.r.t. $\mathbf{P}$ as convex constraint in (83). To this end, (11c) can also be converted into a matrix form. Likewise, we have asymptotic form of (64) w.r.t. $\mathbf{P}$ with an additional generic constraint $\mathbf{P}_{k,k} = 1$ since phase-shift variable is with unit amplitude. Similar to problem (32), we employ a matrix-based PCCP for RIS phase-shift constraint, i.e., $|\mathbf{P}_{k,k'}|^2 \leq a_{k_c} + 1$ and $|\mathbf{P}_{k,k'}|^2 \geq b_{k_c} + 1, \forall k \in \{1, ..., K-1\}, k' \in \{k+1, ..., K\}, k_c = (2K-k)(k-1)/2 + k' - k$. Since the latter constraint is non-convex, we adopt SCA to transform it into convex set as $\mathrm{Re}\{(\mathbf{P}_{k,k'}^*)^{(q)}\mathbf{P}_{k,k'}\} \geq 1 - b_{k_c}$ with the solution at previous q-th iteration. For PCCP, we define the slake variables $\mathbf{a}_r = [a_1, a_2, ..., a_{N_q}] \in \mathbb{R}^{N_q}$ and $\mathbf{b}_r = [b_1, b_2, ..., a_{N_q}] \in \mathbb{R}^{N_q}$ with $N_q = \frac{K(K-1)}{2}$. According to the above transformations, we can reformulate the subproblem (79) as

$$\max_{\mathbf{P}, \overline{\boldsymbol{\gamma}}_D, \mathbf{M}_{\theta,x}, \boldsymbol{\nu}_x, \boldsymbol{\rho}, \mathbf{a}_r, \mathbf{b}_r, \forall x \in \{m,U\}} \sum_{m \in \mathcal{M}} \overline{\gamma}_{D,m} - \lambda^{(q)} \sum_{k_c=1}^{N_q} (a_{k_c} + b_{k_c}) \tag{84a}$$

$$\text{s.t. } \mathbf{M}_{\theta,x} \succeq 0, \quad \nu_{\theta,x} + \frac{1}{\nu_{\theta,x}} \mathrm{Tr}\left(\boldsymbol{\Omega}_{\theta,x}\mathbf{M}_{\theta,x}\right) \leq 0, \quad \forall x \in \{m, U\}, \tag{84b}$$

$$\mathbf{Z}_{t_{\theta,m}}(\mathbf{P}, \mathbf{M}_{\theta,m}, \nu_m) - \left[\begin{array}{cc} \mathbf{0} & \mathbf{0} \\ \mathbf{0} & c_{\rho,m} \end{array}\right] \succeq 0, \quad \forall x \in \{m, U\}, \tag{84c}$$

$$\boldsymbol{\rho} = \{\rho_{1,\theta,x}, \rho_{2,\theta,x}\}, \ \rho_{1,\theta,x} \geq 0, \ \rho_{2,\theta,x} \geq 0, \quad \forall x \in \{m, U\}, \tag{84d}$$

$$\mathbf{P} \succeq 0, \ \mathrm{rank}\left(\mathbf{P}\right) = 1, \ \mathbf{P} = \mathbf{P}^{\mathcal{H}}, \ \mathbf{P}_{k,k} = 1, \forall k \in \mathcal{K}, \tag{84e}$$

$$|\mathbf{P}_{k,k'}|^2 \leq a_{k_c} + 1, \quad \forall k \in \{1, ..., K-1\}, k' \in \{k+1, ..., K\}, k_c = (2K-k)(k-1)/2 + k' - k, \tag{84f}$$

Algorithm 2: Proposed RAPB Scheme with Imperfect CSI

Initialize random active/passive beamforming $\mathbf{W}^{(0)}$ and $\boldsymbol{\theta}^{(0)}$
Set iteration of outer loop $i = 1$
repeat {Outer Loop}
  (BS Active Beamforming):
  Set inner iteration $p = 1$ and $\mathbf{W}_t^{(0)} = \mathbf{W}^{(i-1)}$
  repeat {BS Loop}
    for $m = 1, ..., M$ **do**
      Solve problem (65) for $\mathbf{W}_{t,m}^{(p)}$ with fixed $\boldsymbol{\theta}^{(i-1)}$ and $\mathbf{W}_{t,m'}^{(p-1)}, \forall m' \in \mathcal{M} \backslash m$
    end for
    Update iteration $p \leftarrow p + 1$
  until Convergence of $\mathbf{W}_t$
  Obtain $\mathbf{W}_t^* = \mathbf{W}_t^{(p-1)}$ and decouple it into the vector solution $\mathbf{w}_t^*$
  (RIS Passive Beamforming):
  Set inner iteration $q = 1$ and $\boldsymbol{\theta}_t^{(0)} = \boldsymbol{\theta}^{(i-1)}$, $\kappa \geq 0$, $\lambda^{(0)} = 1$ and $\lambda_{\max}$
  repeat {RIS Loop}
    Solve problem (84) for $\mathbf{P}^{(q)}$ with fixed $\mathbf{w}_t^*$
    Update $\lambda^{(q)} = \min\left\{\kappa\lambda^{(q-1)}, \lambda_{\max}\right\}$.
    Update iteration $q \leftarrow q + 1$
  until Convergence of $\mathbf{P}$
  Obtain $\mathbf{P}^* = \mathbf{P}^{(q-1)}$ and decouple it into a vector form $\boldsymbol{\theta}_t^*$
  Acquire $\left\{\boldsymbol{\theta}^{(i)}, \mathbf{W}^{(i)}\right\} = \{\boldsymbol{\theta}_t^*, \mathbf{W}_t^*\}$
  Update iteration $i \leftarrow i + 1$
until Convergence of total solution
return $\{\boldsymbol{\theta}^*, \mathbf{W}^*\} = \left\{\boldsymbol{\theta}^{(i-1)}, \mathbf{W}^{(i-1)}\right\}$.

$$\mathrm{Re}\{(\mathbf{P}_{k,k'}^*)^{(q)}\mathbf{P}_{k,k'}\} \geq 1 - b_{k_c},\ \forall k \in \{1, ..., K-1\}, k' \in \{k+1, ..., K\}, k_c = (2K-k)(k-1)/2 + k' - k. \tag{84g}$$

The UL/DL constraints from (84b) to (84d) perform convex constraints with LMI property. In (84e), we adopt the same mechanism as problem (65) by dropping the non-convex rank-one constraint of $\mathrm{rank}(\mathbf{P}) = 1$, which results in a solvable SDP problem. Moreover, both PCCP constraints (84f) and (84g) are convex. Therefore, the problem (84) without rank-one constraint is convex, where the optimum of RIS phase-shifts can be readily obtained with arbitrary convex optimization tools. The overall procedure of RAPB is elaborated in Algorithm 2. In RAPB, there is a slight difference compared to APB in terms of the optimization procedure. In RAPB, the BS beamforming is iteratively optimized for each DL UE individually in problem (65), whilst the RIS configuration is represented by the matrix form of $\mathbf{P}$ in problem (84).

V. Performance Evaluation

We evaluate the proposed APB and PAPB schemes for perfect and imperfect CSI cases, respectively. In an RIS-FD transmission system, we consider the Rician channel for all links, i.e., $\sqrt{\frac{1}{\Lambda}}\left(\sqrt{\frac{\varepsilon}{1+\varepsilon}}\mathbf{H}_{\mathrm{LoS}}\right.$

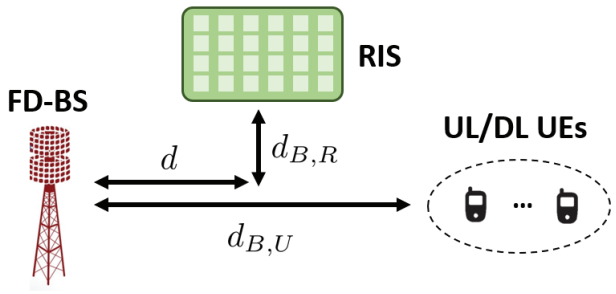

Fig. 4. The scenario of RIS deployment with distances between FD-BS, RIS, and UL/DL UEs.

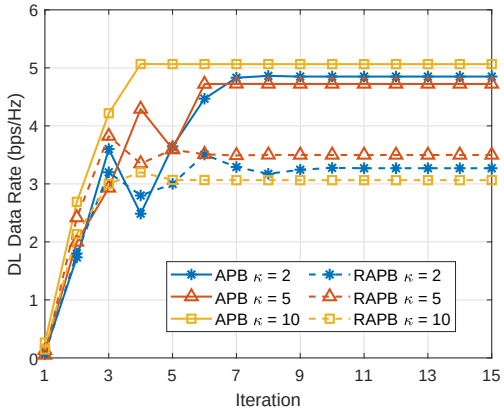

Fig. 5. Convergence of the proposed APB and RAPB schemes with different $\kappa \in \{2, 5, 10\}$ and variance of imperfect CSI $\delta = 0.02$.

TABLE I
PARAMETER SETTING

System Parameters	Value
Carrier frequency	3.5 GHz
Bandwidth	20 MHz
Total transmit power of BS	30 dBm
Total transmit power per UL UE	20 dBm
Noise power spectral density	-174 dBm/Hz
RIS reflection efficiency	0.95
Rician factor	2
Outage probability thresholds of UL/DL	0.9, 0.9
Horizontal distance of BS-RIS/BS-UE	100, 200 m
Perpendicular distance of BS-RIS	100 m

$+\sqrt{\frac{1}{1+\varepsilon}}\mathbf{H}_{\text{NLoS}}\Big)$. The notation Λ is the pathloss of 3.5 GHz frequency bands [46] following $\Lambda = 38.88 + 22\log_{10}(d_0)$ (dB) with d_0 as the distance between either BS-RIS, RIS-UE or BS-UE. ε denotes the Rician factor. $\mathbf{H}_{\text{LoS}}$ is the deterministic line-of-sight (LoS) channel component, whereas $\mathbf{H}_{\text{NLoS}}$ is the random non-line-of-sight (NLoS) model following Rayleigh fading as an exponential distribution with expectation set as one. The simulated scenario is shown in Fig. 4. d, $d_{B,U}$ are defined as the horizontal distance between BS-RIS and BS-UE, respectively. While $d_{B,R}$ indicates the perpendicular distance of BS-RIS. All UL/DL UEs are uniformly distributed in a circular range with a radius of 50 m. Note that we consider a imperfect reflective RIS with reflection efficiency as $\beta = \beta_k = 0.9, \forall k \in \mathcal{K}$. The remaining parameters are listed in Table I.

A. Convergence

In Fig. 5, we evaluate the convergence in terms of total DL data rate of the proposed APB and RAPB schemes with different $\kappa \in \{2, 5, 10\}$ given $N_r = N_t = 6$, $N = M = 4$, $K = 4$, UL SINR threshold

of $\gamma_U = 5$ dB. In order to be consistent for UL QoS, $\overline{t}_{th,U}$ is readily transferred from rate into SINR threshold with logarithmic operation. The iteration here indicates the outer loop of Algorithms 1 and 2. Note that κ represents the increase rate of PCCP penalty of $\lambda^{(q)}$. Intuitively, APB with better channel quality achieves comparably higher DL rate performance than RAPB. We can observe that APB achieves faster convergence than RAPB due to better channel quality of perfect CSI. That is, RAPB requires a comparably complex mechanism to attain robust beamforming than that of APB scheme. In APB, larger κ provides faster convergence as well as the highest data rate since it allows for the optimal determination of the RIS phase variables under perfect CSI. However, the rate performance of RAPB with $\kappa = 10$ is compromised as it requires a slower search rate for the RIS configuration under imperfect CSIs.

B. UL/DL Data Rates with Different Numbers of UL/DL UEs

In Fig. 6, we demonstrate respective UL and DL data rates of our proposed APB and RAPB schemes w.r.t different numbers of DL and UL UEs with $K = 2$, $N_r = N_t = 6$, $\gamma_U \in \{5, 10\}$ dB. Note that we consider $N = 4$ UL UEs when evaluating different numbers of DL UEs. Conversely, we have $M = 4$ DL UEs when evaluating different numbers of UL UEs. Variance of imperfect CSI is set as $\delta = 0.02$. Note that the term "Perfect" in the label of figures means APB scheme with perfect CSI condition. We can observe from all figures that lower γ_U provides higher degree of freedom for DL UEs, resulting in comparatively higher DL rate performance when $\gamma_U = 5$ dB that that of $\gamma_U = 10$ dB. In Figs. 6(a) and 6(b), higher DL rate is achieved with more DL UEs. Nevertheless, the DL rate significantly decreases as the number of UL UEs increases due to the presence of severe co-channel interference from UL UEs. The system prioritizes the DL objective at the expense of UL rate, while ensuring the minimum required UL QoS. In Figs. 6(c) and 6(d), we can observe that the UL rate performance is guaranteed to meet the predefined thresholds. Moreover, they reveal a reverse trend of curves from those in Figs. 6(a) and 6(b). More DL UEs potentially induce higher SI interference reflected from RIS, which leads to a decrease in UL rate performance.

C. Different Numbers of RIS Elements and BS Antennas

Fig. 7 demonstrates the performance of total data rate of APB for perfect CSI and RAPB for imperfect CSI of $\delta = 0.02$, $N_r = N_t = 6$, $M = N = 4$ and different UL QoS thresholds $\gamma_U = \{5, 10, 15, 20\}$ dB. With more RIS elements equipped, the rate escalates thanks to higher degree of freedom of channel diversity. We can find a rate degradation of around 0.1 bps/Hz from perfect CSI to imperfect one. Moreover, higher QoS demands of γ_U lead to stringent service for DL users, having a comparably lower rate of around 7.8 bps/Hz with 18 RIS elements and $\gamma_U = 20$ dB for imperfect CSI. Fig. 8 shows the rate performance of the proposed APB/RAPB schemes with different numbers of BS transmit and receiving antennas. Note that $N_t = 6$ is considered when we evaluate different N_r, and vice versa for $N_r = 6$ when evaluating N_t. We can

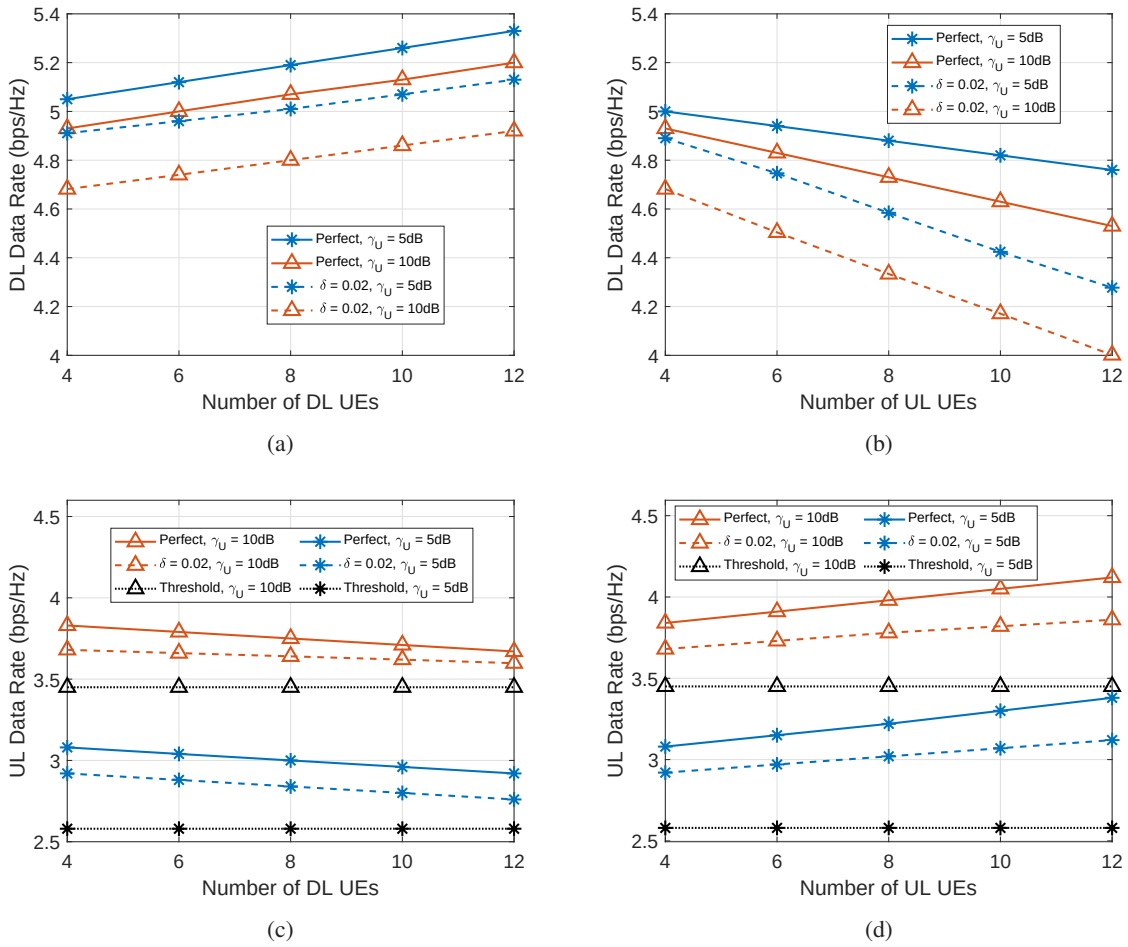

Fig. 6. Performance of DL data rate versus different numbers of (a) DL UEs and (b) UL UEs, and that of UL data rate versus different numbers of (c) DL UEs and (d) UL UEs with UL QoS threshold $\gamma_U \in \{5, 10\}$ dB and variance of imperfect CSI $\delta = 0.02$.

observe that the total data rate increases as the number of transmit antennas is increased. This is because having more transmit antennas enables higher channel diversity, which results in enhanced beamforming and reduced interference for DL UEs. As a result, the system can support a larger number of users with higher data rate. On the other hand, we notice that increasing the number of RIS elements from $K = 16$ to $K = 32$ leads to an insignificant rate improvement of rate, which implies that adding more RIS elements does not provide additional benefits in terms of channel diversity for DL users. In other words, the existing RIS elements of $K = 16$ is sufficient to serve the DL UEs effectively. On the other hand, we observe a decreased rate as the number of receiving antennas is increased. This is because more antennas induce more interferences from both the BS transmit antennas and the reflecting signals from the RIS. In order to simultaneously mitigate SI and ensure reliable UL UE service, the RIS has to dedicate its elements to eliminating the interference, which in turn affects the DL service and leads to degraded data rate. Therefore, it becomes a compelling tradeoff between UL and DL performance in a full-duplex system with different numbers of transmit/receiving antennas.

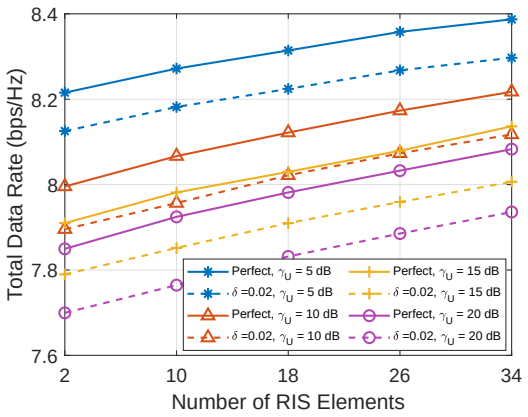

Fig. 7. Total data rate versus different numbers of RIS elements w.r.t. UL QoS thresholds $\gamma_U \in \{5, 10, 15, 20\}$ dB.

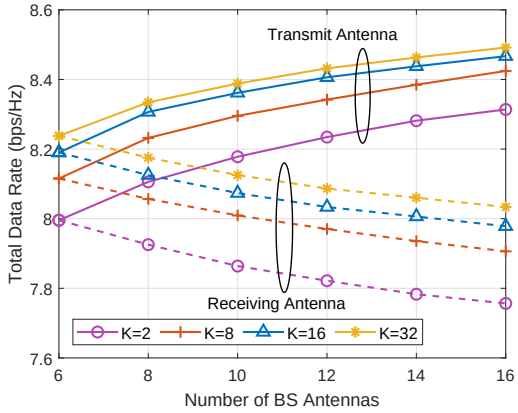

Fig. 8. Total data rate versus different numbers of BS transmit antennas and receiving antennas w.r.t. RIS elements $K \in \{2, 8, 16, 32\}$.

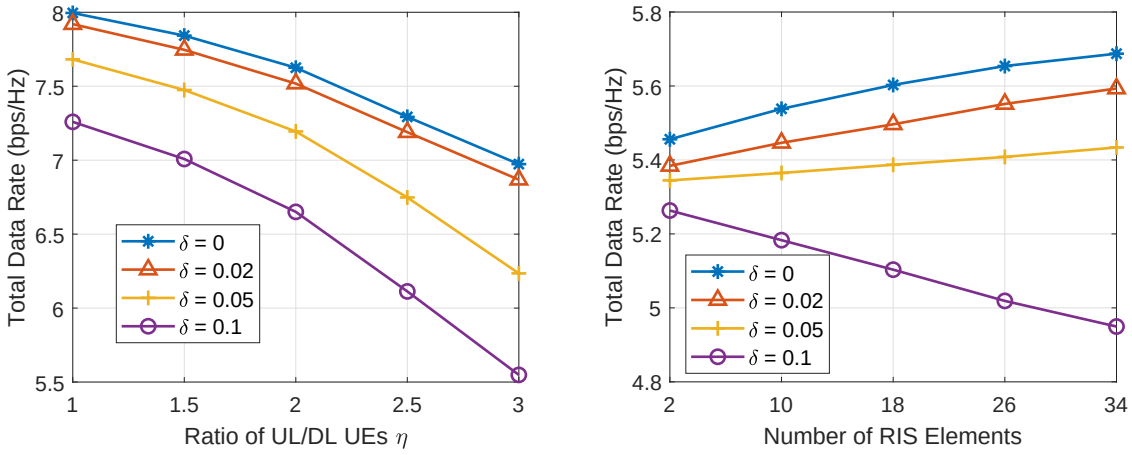

(a) (b)

Fig. 9. Total data rates versus (a) different ratios of number of UL UEs to DL UEs η and (b) different numbers of RIS elements w.r.t. imperfect CSI variance as $\delta \in \{0, 0.02, 0.05, 0.1\}$.

D. Effect of Imperfect CSI

In Fig. 9, we demonstrate the effect of imperfect CSI for the proposed RAPB scheme with $\gamma_U = 5$ dB, $N_t = N_r = 6$ and $\gamma \in \{0, 0.02, 0.05, 0.1\}$. In Fig. 9(a), we consider different ratios of the number of UL UEs to DL UEs $\eta \in \{1, 1.5, 2, 2.5, 3\}$. As explained previously, the increased number of UL UEs results in a greater allocation of resources to meet the UL QoS requirements at the expense of the DL data rate. Specifically, when considering the largest channel error variance of $\delta = 0.1$, we can observe a decrease in the data rate from approximately 7.3 to 5.5 bps/Hz. Furthermore, it is worth noting that higher channel error variances lead to even lower data rates, indicating the impact of channel uncertainties on the overall RIS-aided system. In Fig. 9(b), we evaluate the effect of imperfect CSI with different numbers of RIS elements. With smaller channel error of $\delta = 0.02$, it still performs the similar increasing trend as that of perfect case

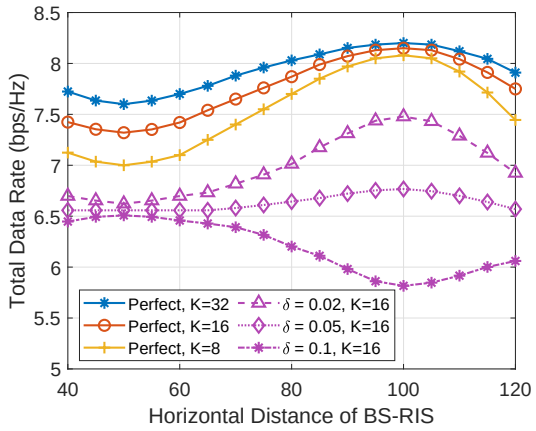

Fig. 10. Total data rates versus different deployed horizontal distance between BS-RIS for perfect and imperfect CSI. Note that different numbers of RIS elements $K \in \{8, 16, 32\}$ are considered in APB, whilst different error variance $\delta \in \{0.02, 0.05, 0.1\}$ with $K = 16$ is for RAPB.

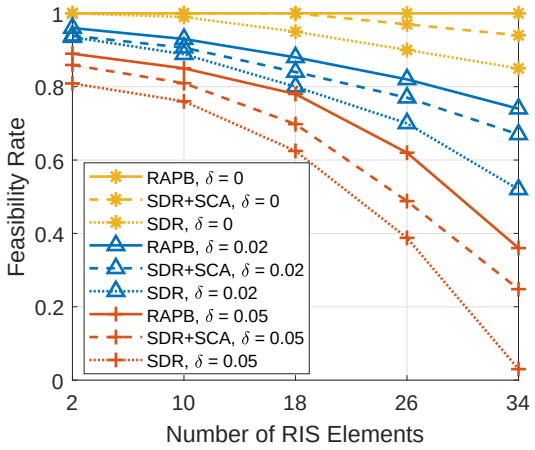

Fig. 11. Performance comparison of the feasibility rate of proposed RAPB to SDR-based SCA and pure SDR methods w.r.t. different numbers of RIS elements and channel error variance $\delta \in \{0, 0.02, 0.05\}$.

with $\delta = 0$. However, when the channel error escalates from $\delta = 0.02$ to $\delta = 0.05$, a comparably smaller rate improvement is observed. Intriguingly, for $\delta = 0.1$, the rate performance exhibits a different trend with a noticeable decline of rate. This decline can be attributed to the increased severity of random channel errors. As the number of RIS elements increases, the quality of the RIS channel deteriorates, making it more challenging to achieve effective beamforming.

E. Impact of RIS Deployment

Fig. 10 illustrates the performance of deployment under perfect and imperfect CSI w.r.t. different horizontal distances between BS-RIS $d \in [40, 120]$ m given $N_r = N_t = 6$, $M = N = 4$ and $\gamma_U = 5$ dB. For the case of perfect CSI, we consider different RIS elements of $K \in \{8, 16, 32\}$ for APB. While different variance values of channel error $\delta \in \{0.02, 0.05, 0.1\}$ are for RAPB. We can observe three curve trends when $d \leq 100$ m, $d = 100$ m, and $d \geq 100$ m. If d is smaller than 100 m, the benefit of RIS deployment near the BS is high thanks to more desired reflected signal power and cancellation of severe interference. However, UL signals may be weak before it reaches the RIS. Moreover, they perform a convex shape with minimum rate at $d = 50$ m since the RIS is capable of more focusing on guaranteeing the reflected signals of UL at the expense of DL UEs. As for $d \in [50, 100]$ m, increasing the deployment distance of d provides a shorter total distance of BS-RIS and RIS-UE. The optimal deployment of the RIS can be achieved when the distance $d = 100$ m between BS-RIS, which corresponds to the midpoint between the BS-RIS and RIS-UE. By appropriately placing the RIS at this optimal location, it can effectively mitigate interference and enhance the desired signal power with the significant rate improvement. When d goes beyond 100 m, the pathloss will dominate the result, which results in a decreasing data rate performance. Moreover, once the RIS is

optimally deployed, even a smaller size of RIS will become sufficient to support both UL/DL UEs. When we consider imperfect CSI for deployment, it has different trends than that of perfect case. Smaller channel error $\delta = 0.02$ possesses the asymptotically similar trend to that with perfect CSI. When $\delta = 0.05$, the benefit of deployment becomes less significant, i.e., better RIS configuration and estimation mechanism will be much more important than the appropriate deployment. Intriguingly, the opposite performance can be observed when the sufficiently-high channel error $\delta = 0.1$ take place. This phenomenon arises due to the severe impact of channel errors on both the BS-RIS and the RIS-UE links when the RIS is located at a optimal point with $d = 100$ m. Both links are significantly affected by channel errors, resulting in erroneous channel estimation. However, as a remedy, the stronger path between either the BS-RIS or RIS-UE link can partially compensate for the channel errors, resulting in a moderate data rate performance.

F. Comparison of Benchmarks

In Fig. 11, we evaluate the feasibility rate of RAPB with the existing algorithms considering different numbers of RIS elements with error variance $\delta \in \{0, 0.02, 0.05\}$, $K = 4$, $N_r = N_t = 6$, $M = N = 4$ and $\gamma_U = 5$ dB. The feasibility rate is defined as the percentage of the number of feasible solutions over the total channel realization, i.e., how many solution can satisfy the constraints. We consider two algorithm benchmarks including the conventional SDR [47] and the SDR-based SCA method [48]. In RAPB, SDR and SCA as well as penalty CCP are employed. We can observe that smaller channel errors provide more feasible solutions satisfying the service requirement. As explained previously, more RIS elements with imperfect CSI have comparably larger errors leading to unsatisfying solutions, i.e., lower than half solutions can support the service when $\delta = 0.05$ and $K = 34$ RIS elements. For the pure SDR method, the solution is not constrained only by the rank-1 matrix, which results in lots of solutions inappropriate. The method of SDR+SCA has further constraints of linearization of RIS phase-shifts in (84g) but without penalties in objective (84a), which achieves higher feasibility rate than pure SDR. Benefited by additional penalty in PCCP, the proposed RAPB achieves the highest feasibility rate among other algorithms.

In Fig. 12, we compare the proposed APB and RAPB schemes to different robust/non-robust benchmarks with $\delta = 0.02$, $K = 4$, $N_r = N_t = 6$ and $\gamma_U = 5$ dB. Note that the APB refers to the optimal solution with perfect CSI case. Robust SDR indicates that SDR [47] is applied with imperfect CSI considering only dropping rank-1 matrix. Moreover, non-robust based methods represent that they directly adopt the estimated erroneous CSI to optimize the BS/RIS beamforming without further process. We can observe that the proposed RAPB asymptotically approaches the optimal solution with perfect CSI since it is capable of well dealing with uncertainty of RIS channels. As explained in Fig. 11, SDR without penalized RIS phase-shift auxiliary parameters cannot provide feasible solutions even though it is robust to RIS channel

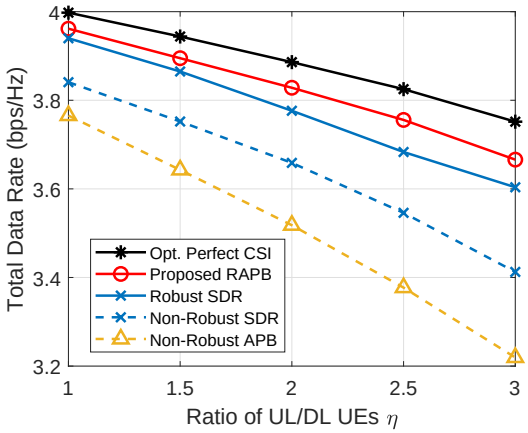

Fig. 12. Performance comparison of the proposed RAPB scheme with optimal APB under perfect CSI, robust/non-robust SDR and non-robust APB w.r.t. different ratios of UL/DL UEs η.

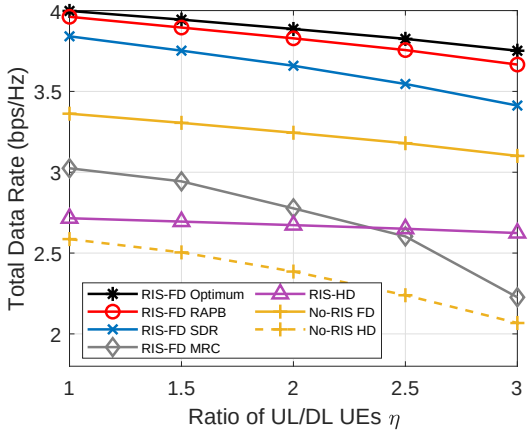

Fig. 13. Performance comparison of the proposed APB/RAPB schemes with SDR, MRC, HD, and non-RIS deployment under robustness case with imperfect CSI w.r.t. different ratios of UL/DL UEs η.

imperfection. As for non-robust case, we can observe that directly using APB under imperfect CSI will have a severe degradation of rate with around 25% loss compared to SDR when $\eta = 3$.

In Fig. 13, we compare the proposed RAPB scheme to the existing methods under robustness case of imperfect CSI: (1) Maximum ratio combining (**MRC**) method [49] is applied in active/passive beamforming. (2) **RIS-HD** [50] considers the service in a DL-only system, i.e., no UL signal interference as well as UL QoS constraint. (3) **No-RIS FD/HD** indicates that there exists no deployment of RIS under conventional FD [17] and HD [35] scenarios. We can that it has the worst data rate for HD service without the assistance of RIS due to insufficient channel diversity. With the benefit of RIS, RIS-HD improves around 30% rate performance compared to No-RIS HD case when $\eta = 3$. Moreover, No-RIS FD technique can fully utilize spectrum, which provides additional 20% total rate than that of HD case. The conventional MRC method applied both in active and passive beamforming cannot well resolve the complex interference including SI and CCI under imperfect CSI, which has even worse rate than that without RIS deployment. With the utilization of SDR optimization, it reaches a rate improvement of around 48% compared to RIS-FD MRC. With consideration of imperfect CSI as well as penalty-based RIS solution, the proposed RAPB can achieve the highest data rate performance among the other benchmarks and asymptotically approach the optimal APB case in perfect CSI.

VI. Conclusions

In this paper, we have proposed APB and RAPB schemes for optimizing active BS and passive RIS beamforming under perfect and imperfect CSI of RIS channels, respectively. The objective is to maximize the total DL rate while satisfying the UL QoS requirements. In APB, we employ Lagrangian dual, Dinkelbach,

and AO algorithms to decouple the active/passive beamforming problem into two convex sub-problems. In RAPB, we introduce distributionally robust optimization with CVaR transformation, whilst LMI is leveraged to reformulate two decoupled convex sub-problems. Both schemes utilize PCCP for the constraint on RIS phase-shifts. In simulations, APB achieves a higher rate compared to RAPB due to the availability of perfect CSI. We also observe that higher number of RIS elements or BS antennas can improve the rate thanks to increasing channel diversity. When channel error is larger, adding more RIS elements might lead to a non-intuitive rate degradation. The optimal RIS deployment is envisioned through simulation. Moreover, RAPB has the highest solution feasibility rate than the other methods of SDR and SCA. In conclusion, the proposed APB and RAPB schemes have revealed superior datae rate performance to the other existing methods in terms of non-robustness, SDR, conventional beamforming, RIS-HD, and non-RIS deployment.

REFERENCES

[1] Y. Liu, X. Liu, X. Mu, T. Hou, J. Xu, M. Di Renzo, and N. Al-Dhahir, "Reconfigurable intelligent surfaces: Principles and opportunities," *IEEE Communications Surveys and Tutorials*, vol. 23, no. 3, pp. 1546–1577, 2021.

[2] P. Tulupov, B. Sorokin, and A. Korolev, "Coverage impact of reconfigurable intelligent surfaces in 6G mobile networks," in *Proc. International Conference on Electrical, Computer and Energy Technologies (ICECET)*, 2022, pp. 1–5.

[3] L.-H. Shen, K.-T. Feng, and L. Hanzo, "Five facets of 6G: Research challenges and opportunities," *ACM Computing Surveys*, vol. 55, no. 11, pp. 1–39, 2023.

[4] C. Pan, H. Ren, K. Wang, J. F. Kolb, M. Elkashlan, M. Chen, M. Di Renzo, Y. Hao, J. Wang, A. L. Swindlehurst, X. You, and L. Hanzo, "Reconfigurable intelligent surfaces for 6G systems: Principles, applications, and research directions," *IEEE Communications Magazine*, vol. 59, no. 6, pp. 14–20, 2021.

[5] Y. Cao, T. Lv, W. Ni, and Z. Lin, "Sum-rate maximization for multi-reconfigurable intelligent surface-assisted device-to-device communications," *IEEE Transactions on Communications*, vol. 69, no. 11, pp. 7283–7296, 2021.

[6] T. Hou, Y. Liu, Z. Song, X. Sun, Y. Chen, and L. Hanzo, "Reconfigurable intelligent surface aided NOMA networks," *IEEE Journal on Selected Areas in Communications*, vol. 38, no. 11, pp. 2575–2588, 2020.

[7] A. Al-Hilo, M. Samir, M. Elhattab, C. Assi, and S. Sharafeddine, "Reconfigurable intelligent surface enabled vehicular communication: Joint user scheduling and passive beamforming," *IEEE Transactions on Vehicular Technology*, vol. 71, no. 3, pp. 2333–2345, 2022.

[8] Y. Liu, Z. Su, C. Zhang, and H.-H. Chen, "Minimization of secrecy outage probability in reconfigurable intelligent surface-assisted MIMOME system," *IEEE Transactions on Wireless Communications*, pp. 1–1, 2022.

[9] J. Ye, S. Guo, and M.-S. Alouini, "Joint reflecting and precoding designs for SER minimization in reconfigurable intelligent surfaces assisted MIMO systems," *IEEE Transactions on Wireless Communications*, vol. 19, no. 8, pp. 5561–5574, 2020.

[10] P. Wang, J. Fang, X. Yuan, Z. Chen, and H. Li, "Intelligent reflecting surface-assisted millimeter wave communications: Joint active and passive precoding design," *IEEE Transactions on Vehicular Technology*, vol. 69, no. 12, pp. 14 960–14 973, 2020.

[11] H. Chen, G. Yang, and Y.-C. Liang, "Joint active and passive beamforming for reconfigurable intelligent surface enhanced symbiotic radio system," *IEEE Wireless Communications Letters*, vol. 10, no. 5, pp. 1056–1060, 2021.

[12] Z. Tang, T. Hou, Y. Liu, J. Zhang, and C. Zhong, "A novel design of RIS for enhancing the physical layer security for RIS-aided NOMA networks," *IEEE Wireless Communications Letters*, vol. 10, no. 11, pp. 2398–2401, 2021.

[13] M. Almekhlafi, M. A. Arfaoui, M. Elhattab, C. Assi, and A. Ghrayeb, "Joint resource allocation and phase shift optimization for RIS-aided eMBB/URLLC traffic multiplexing," *IEEE Transactions on Communications*, vol. 70, no. 2, pp. 1304–1319, 2022.

[14] W. Tang, M. Z. Chen, X. Chen, J. Y. Dai, Y. Han, M. Di Renzo, Y. Zeng, S. Jin, Q. Cheng, and T. J. Cui, "Wireless communications with reconfigurable intelligent surface: Path loss modeling and experimental measurement," *IEEE Transactions on Wireless Communications*, vol. 20, no. 1, pp. 421–439, 2021.

[15] H. Wymeersch, J. He, B. Denis, A. Clemente, and M. Juntti, "Radio localization and mapping with reconfigurable intelligent surfaces: Challenges, opportunities, and research directions," *IEEE Vehicular Technology Magazine*, vol. 15, no. 4, pp. 52–61, 2020.

[16] J. Xu, Y. Liu, X. Mu, and O. A. Dobre, "STAR-RISs: Simultaneous transmitting and reflecting reconfigurable intelligent surfaces," *IEEE Communications Letters*, vol. 25, no. 9, pp. 3134–3138, 2021.

[17] C.-H. Fang, P.-R. Li, and K.-T. Feng, "Joint interference cancellation and resource allocation for full-duplex cloud radio access networks," *IEEE Transactions on Wireless Communications*, vol. 18, no. 6, pp. 3019–3033, 2019.

[18] C.-H. Fang and K.-T. Feng, "Queue-aware beam assignment and rate control for time-varying mm-wave-based full-duplex small cell networks," *IEEE Communications Letters*, vol. 24, no. 1, pp. 222–226, 2020.

[19] T. Riihonen, A. Balakrishnan, K. Haneda, S. Wyne, S. Werner, and R. Wichman, "Optimal eigenbeamforming for suppressing self-interference in full-duplex MIMO relays," in *Proc. Annual Conference on Information Sciences and Systems (CISS)*, 2011, pp. 1–6.

[20] S. Arzykulov, G. Nauryzbayev, A. Celik, and A. M. Eltawil, "RIS-assisted full-duplex relay systems," *IEEE Systems Journal*, vol. 16, no. 4, pp. 5729–5740, 2022.

[21] R. Deshpande, M. Katwe, K. Singh, and Z. Ding, "Resource allocation design for spectral-efficient URLLC using RIS-aided FD-NOMA system," *IEEE Wireless Communications Letters*, pp. 1–1, 2023.

[22] Y. Wang, P. Guan, H. Yu, and Y. Zhao, "Transmit power optimization of simultaneous transmission and reflection RIS assisted full-duplex communications," *IEEE Access*, vol. 10, pp. 61 192–61 200, 2022.

[23] F. Karim, B. Hazarika, S. K. Singh, and K. Singh, "A performance analysis for multi-ris-assisted full duplex wireless communication system," in *Proc. IEEE International Conference on Acoustics, Speech and Signal Processing (ICASSP)*, 2022, pp. 5313–5317.

[24] Z. Peng, Z. Zhang, C. Pan, L. Li, and A. L. Swindlehurst, "Multiuser full-duplex two-way communications via intelligent reflecting surface," *IEEE Transactions on Signal Processing*, vol. 69, pp. 837–851, 2021.

[25] Z. Peng, Z. Chen, C. Pan, G. Zhou, and H. Ren, "Robust transmission design for RIS-aided communications with both transceiver hardware impairments and imperfect CSI," *IEEE Wireless Communications Letters*, vol. 11, no. 3, pp. 528–532, 2022.

[26] H. Gao, K. Cui, C. Huang, and C. Yuen, "Robust beamforming for RIS-assisted wireless communications with discrete phase shifts," *IEEE Wireless Communications Letters*, vol. 10, no. 12, pp. 2619–2623, 2021.

[27] Y. Chen, Y. Wang, and L. Jiao, "Robust transmission for reconfigurable intelligent surface aided millimeter wave vehicular communications with statistical CSI," *IEEE Transactions on Wireless Communications*, vol. 21, no. 2, pp. 928–944, 2022.

[28] G. Zhou, C. Pan, H. Ren, K. Wang, and A. Nallanathan, "A framework of robust transmission design for IRS-aided MISO communications with imperfect cascaded channels," *IEEE Transactions on Signal Processing*, vol. 68, pp. 5092–5106, 2020.

[29] L. Zhang, C. Pan, Y. Wang, H. Ren, and K. Wang, "Robust beamforming design for intelligent reflecting surface aided cognitive radio systems with imperfect cascaded CSI," *IEEE Transactions on Cognitive Communications and Networking*, vol. 8, no. 1, pp. 186–201, 2022.

[30] Y. Xu, H. Xie, Q. Wu, C. Huang, and C. Yuen, "Robust max-min energy efficiency for RIS-aided hetnets with distortion noises," *IEEE Transactions on Communications*, vol. 70, no. 2, pp. 1457–1471, 2022.

[31] H. Rahimian and S. Mehrotra, "Frameworks and results in distributionally robust optimization," *Open Journal of Mathematical Optimization*, vol. 3, pp. 1–85, 2022.

[32] J. Zhou, W. Liu, X. Chen, M. Sun, C. Mei, S. He, H. Gao, and J. Liu, "A distributionally robust chance constrained planning method for integrated energy systems," in *Proc. IEEE PES Asia-Pacific Power and Energy Engineering Conference (APPEEC)*, 2019, pp. 1–5.

[33] Q. Li, A. M.-C. So, and W.-K. Ma, "Distributionally robust chance-constrained transmit beamforming for multiuser MISO downlink," in *Proc. IEEE International Conference on Acoustics, Speech and Signal Processing (ICASSP)*, 2014, pp. 3479–3483.

[34] X. Liu, Y. Gao, L. Wang, N. Sha, and S. Wang, "Distributionally robust optimization for secure transmission with assisting jammer in MISO downlink networks," *IEEE Communications Letters*, vol. 23, no. 2, pp. 338–341, 2019.

[35] B. Li, M. Zhang, Y. Rong, and Z. Han, "Transceiver optimization for wireless powered time-division duplex MU-MIMO systems: Non-robust and robust designs," *IEEE Transactions on Wireless Communications*, vol. 21, no. 6, pp. 4594–4607, 2022.

[36] C.-J. Ku, L.-H. Shen, and K.-T. Feng, "Reconfigurable intelligent surface assisted interference mitigation for 6G full-duplex MIMO

communication systems," in *Proc. IEEE Annual International Symposium on Personal, Indoor and Mobile Radio Communications (PIMRC)*, 2022, pp. 327–332.

[37] K. Shen and W. Yu, "Fractional programming for communication systems—part ii: Uplink scheduling via matching," *IEEE Transactions on Signal Processing*, vol. 66, no. 10, pp. 2631–2644, 2018.

[38] W. Dinkelbach, "On nonlinear fractional programming," *Management Science*, vol. 13, no. 7, pp. 492–498, 1967.

[39] S. Moazeni, W. B. Powell, and A. H. Hajimiragha, "Mean-conditional value-at-risk optimal energy storage operation in the presence of transaction costs," *IEEE Transactions on Power Systems*, vol. 30, no. 3, pp. 1222–1232, 2015.

[40] S. Zymler, D. Kuhn, and B. Rustem, "Distributionally robust joint chance constraints with second-order moment information," *Mathematical Programming*, vol. 137, no. 1, pp. 167–198, 2013.

[41] R. T. Rockafellar and S. Uryasev, "Optimization of conditional value-at risk," *Journal of Risk*, vol. 3, pp. 21–41, 2000.

[42] A. Shapiro and A. Kleywegt, "Minimax analysis of stochastic problems," *Optimization Methods and Software*, vol. 17, no. 3, pp. 523–542, 2002.

[43] A. M.-C. So, J. Zhang, and Y. Ye, "On approximating complex quadratic optimization problems via semidefinite programming relaxations," *Mathematical Programming*, vol. 110, no. 1, pp. 93–110, 2007.

[44] E. A. Gharavol and E. G. Larsson, "The sign-definiteness lemma and its applications to robust transceiver optimization for multiuser MIMO systems," *IEEE Transactions on Signal Processing*, vol. 61, no. 2, pp. 238–252, 2013.

[45] F. Zhang, *The Schur Complement and Its Applications*. Springer New York, NY, 2005.

[46] 3GPP, "Study on channel model for frequencies from 0.5 to 100 ghz," *TR 38.901 version 15.0.0 Release 15*, 2018.

[47] H. Han, J. Zhao, W. Zhai, Z. Xiong, D. Niyato, M. Di Renzo, Q.-V. Pham, W. Lu, and K.-Y. Lam, "Reconfigurable intelligent surface aided power control for physical-layer broadcasting," *IEEE Transactions on Communications*, vol. 69, no. 11, pp. 7821–7836, 2021.

[48] Y. Chen, Y. Wang, J. Zhang, and Z. Li, "Resource allocation for intelligent reflecting surface aided vehicular communications," *IEEE Transactions on Vehicular Technology*, vol. 69, no. 10, pp. 12 321–12 326, 2020.

[49] J. Ye, A. Kammoun, and M.-S. Alouini, "Spatially-distributed riss vs relay-assisted systems: A fair comparison," *IEEE Open Journal of the Communications Society*, vol. 2, pp. 799–817, 2021.

[50] Y. Liu, Y. Zhang, X. Zhao, S. Geng, P. Qin, and Z. Zhou, "Dynamic-controlled ris assisted multi-user miso downlink system: Joint beamforming design," *IEEE Transactions on Green Communications and Networking*, vol. 6, no. 2, pp. 1069–1081, 2022.